FLUID DYNAMICS IN ASTROPHYSICS AND COSMOLOGY II

Eulerian Gas Dynamics

- **THE EQUATIONS OF GAS DYNAMICS IN EULERIAN FORM (1D):**

$$\frac{\partial \rho}{\partial t} + \frac{\partial (\rho u)}{\partial x} = 0$$

$$\frac{\partial (\rho u)}{\partial t} + \frac{\partial}{\partial x}(\rho u^2 + p) = 0$$

$$\frac{\partial e}{\partial t} + \frac{\partial}{\partial x}(u(e + p)) = 0$$

$$p = (\gamma - 1)\left(e - \frac{1}{2}\rho u^2\right)$$

EULERIAN GAS DYNAMICS

- IN COMPACT VECTOR FORM:

$$\frac{\partial}{\partial t}\mathbf{U} + \frac{\partial}{\partial x}\mathbf{F}(\mathbf{U}) = 0\,,$$

$$\mathbf{U} = \begin{pmatrix} \rho \\ \rho u \\ e \end{pmatrix}\,, \qquad \mathbf{F} = \begin{pmatrix} \rho u \\ \rho u^2 + p \\ u(e+p) \end{pmatrix}$$

$$p = (\gamma - 1)\left(e - \frac{1}{2}\rho u^2\right)$$

- U is a vector of states and F is a vector of fluxes (mass, momentum and energy)

Euler equations in 3D

We can write a general conservation laws in the form

$$\frac{\partial q}{\partial t}+\nabla\cdot\boldsymbol{F}(q,t)=0$$

For example, for the Euler equations we have

$$q=\begin{Bmatrix}\rho\\ \rho u_x\\ \rho u_y\\ \rho u_z\\ \rho E\end{Bmatrix} \qquad \boldsymbol{F}(q)=\begin{Bmatrix}\rho u_x & \rho u_y & \rho u_z\\ \rho u_x^2+P & \rho u_x u_y & \rho u_x u_z\\ \rho u_x u_y & \rho u_y^2+P & \rho u_y u_z\\ \rho u_x u_z & \rho u_y u_z & \rho u_z^2+P\\ (\rho E+P)u_x & (\rho E+P)u_y & (\rho E+P)u_z\end{Bmatrix}$$

Grid based methods

- Discretization of variables in time and space

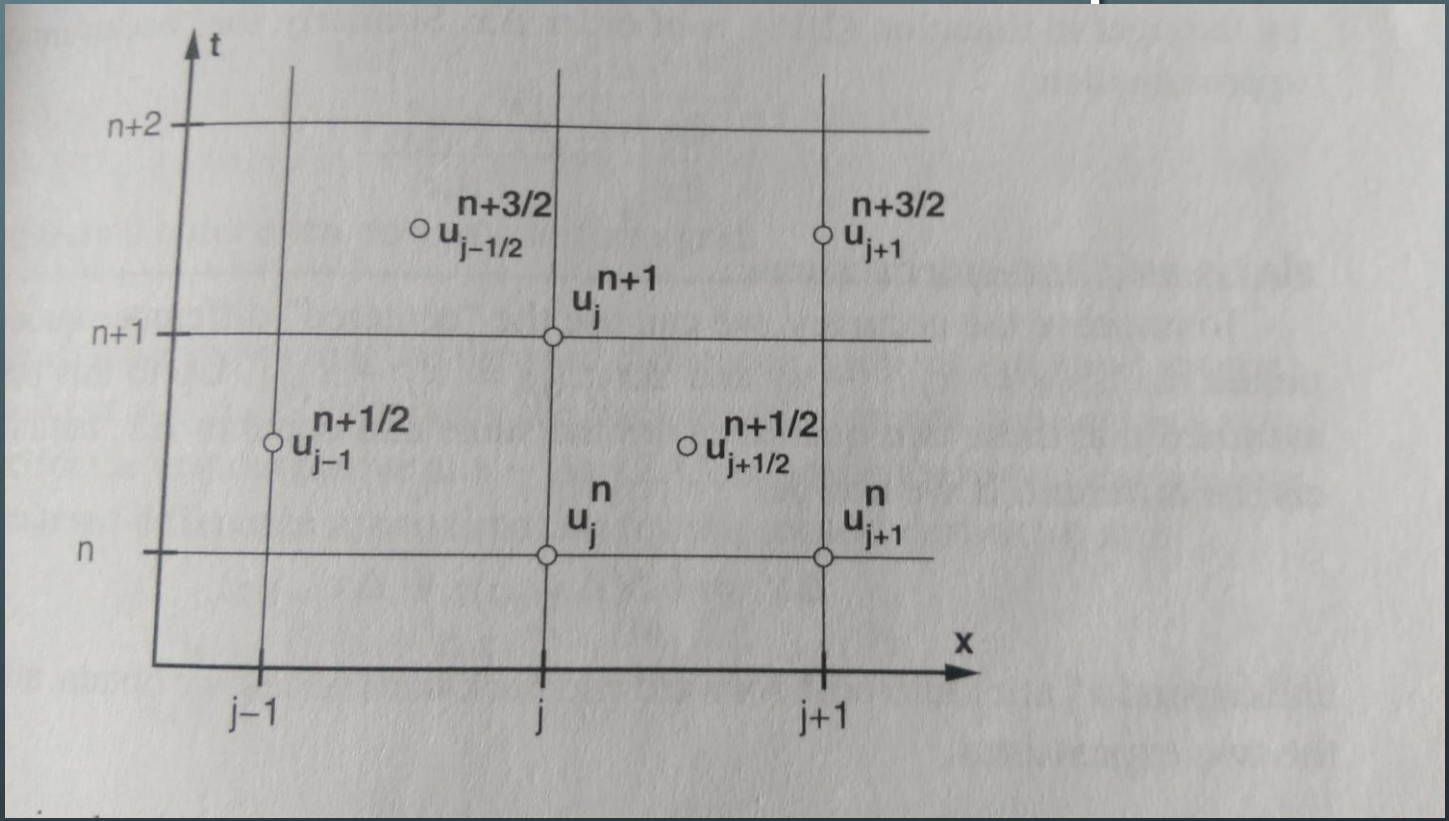

Types of numerical grid based methods

- Finite difference schemes
  - Explicit in time
  - Implicit in time

- Finite Volume schemes:
  - Godunov's zero order method
  - Higher–order Godunov's methods

Explicit finite difference

- **Lax-Wendroff explicit scheme:**

Start with the Taylor expansion in time:

$$\rho_i^{n+1} \equiv \rho(x_i, t_{n+1}) = \rho_i^n + \Delta t \left.\frac{\partial \rho}{\partial t}\right|_i^n + \frac{1}{2}\Delta t^2 \left.\frac{\partial^2 \rho}{\partial t^2}\right|_i^n + O(\Delta t^3)$$

Use the advection equation to obtain exact expressions for the derivatives:

$$\left.\frac{\partial \rho}{\partial t}\right|_i^n = -u \left.\frac{\partial \rho}{\partial x}\right|_i^n \qquad \left.\frac{\partial^2 \rho}{\partial t^2}\right|_i^n = u^2 \left.\frac{\partial^2 \rho}{\partial x^2}\right|_i^n$$

Use centered spatial differences to obtain

$$\rho_i^{n+1} = \rho_i^n - \frac{u\,\Delta t}{2\,\Delta x}\left(\rho_{i+1}^n - \rho_{i-1}^n\right) + \frac{u^2 \Delta t^2}{2\,\Delta x^2}\left(\rho_{i+1}^n - 2\,\rho_i^n + \rho_{i-1}^n\right)$$

This is the *Lax-Wendroff method*. It has second-order truncation error (space and time).

The leading-order error terms are odd in both x and t, so the error is dispersive (produces ripples) rather than diffusive...

Explicit finite difference

- Lax-Wendroff explicit scheme:

$u\Delta t/\Delta x = 0.1$

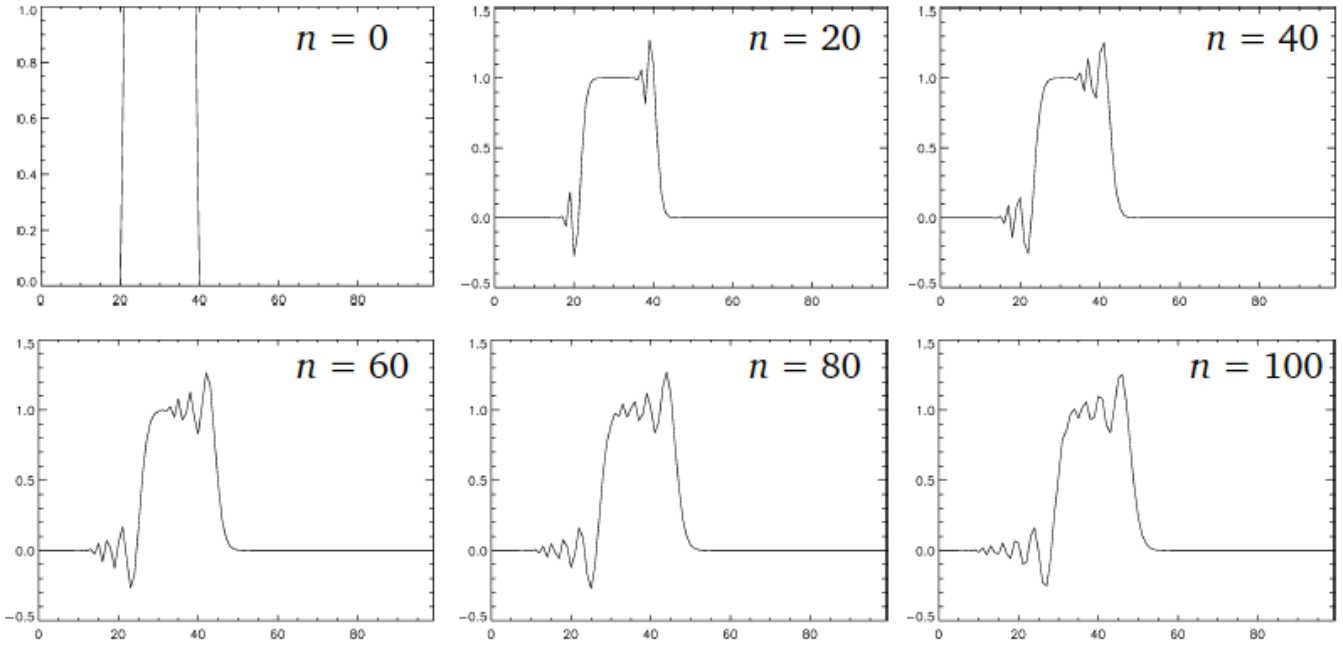

Errors tend to be generated near discontinuities, where the Gibbs phenomenon prevents us from capturing all of the modes in the true continuum solution using a discrete mesh.

Implicit scheme

An *implicit* method uses spatial derivatives evaluated at the updated time t_{n+1}.

An example is the *backward time-centered space method*:

$$\rho_i^{n+1} = \rho_i^n - \frac{u\,\Delta t}{2\,\Delta x}\left(\rho_{i+1}^{n+1} - \rho_{i-1}^{n+1}\right)$$

The difference equation domain of dependence covers the entire grid – so implicit schemes are unconditionally stable. However, for more advanced methods they are generally more difficult to formulate.

Write as a matrix equation for the entire grid:

$$\begin{bmatrix} 1 & \sigma & & & & & \\ -\sigma & 1 & \sigma & & & & \\ & -\sigma & 1 & \sigma & & & \\ & & & \ddots & & & \\ & & & -\sigma & 1 & \sigma & \\ & & & & -\sigma & 1 & \end{bmatrix} \begin{bmatrix} \rho_0^{n+1} \\ \rho_1^{n+1} \\ \rho_2^{n+1} \\ \vdots \\ \rho_{N-1}^{n+1} \\ \rho_N^{n+1} \end{bmatrix} = \begin{bmatrix} \rho_0^n \\ \rho_1^n \\ \rho_2^n \\ \vdots \\ \rho_{N-1}^n \\ \rho_N^n \end{bmatrix}, \qquad \sigma \equiv \frac{u\,\Delta t}{2\,\Delta x}$$

This equation is solved using standard linear algebra techniques.

Note that the boundary conditions are included in the matrix definition.

Higher dimensions

- Operator splitting

Creating multidimensional differencing methods is possible, but complex (especially for implicit methods).

A common workaround is *operator splitting*: suppose we have a difference operator D with truncation error $O(\Delta t)$ or better that can be written

$$D = D_1 + D_2 + D_3$$

Then we can approximate the action of D by composing the operators D_1, D_2, D_3:

$$D[q] = D_1[D_2[D_3[q]]] + O(\Delta t)$$

If D is $O(\Delta t^2)$, we can do better by symmmetrizing the operator:

$$D[q] = D_1^{1/2}[D_2^{1/2}[D_3^{1/2}[D_3^{1/2}[D_2^{1/2}[D_1^{1/2}[q]]]]]] + O(\Delta t^2)$$

This is called *Strang splitting*. Each of the operators is applied for ½ Δt.

Higher dimensions

- Operator splitting

For example, consider linear advection in two dimensions:

$$\frac{\partial \rho}{\partial t} + u_x \frac{\partial \rho}{\partial x} + u_y \frac{\partial \rho}{\partial y} = 0$$

Define the two Lax-Wendroff operators

$$D_x[\rho_{ij}, \Delta t] = \rho_{ij} - \frac{u_x \Delta t}{2\Delta x}\left(\rho_{i+1,j} - \rho_{i-1,j}\right) + \frac{u_x^2 \Delta t^2}{2\Delta x^2}\left(\rho_{i+1,j} - 2\rho_{ij} + \rho_{i-1,j}\right)$$

$$D_y[\rho_{ij}, \Delta t] = \rho_{ij} - \frac{u_y \Delta t}{2\Delta y}\left(\rho_{i,j+1} - \rho_{i,j-1}\right) + \frac{u_y^2 \Delta t^2}{2\Delta y^2}\left(\rho_{i,j+1} - 2\rho_{ij} + \rho_{i,j-1}\right)$$

Then we can create the following second-order 2D method:

$$\rho_{ij}^{(1)} = D_x[\rho_{ij}^n, \Delta t/2]$$
$$\rho_{ij}^{(2)} = D_y[\rho_{ij}^{(1)}, \Delta t/2]$$
$$\rho_{ij}^{(3)} = D_y[\rho_{ij}^{(2)}, \Delta t/2]$$
$$\rho_{ij}^{n+1} = D_x[\rho_{ij}^{(3)}, \Delta t/2]$$

The CFL criterion is applied to each operator separately.
Operator splitting is also used to include different physics, e.g., source terms.

Finite Volume Schemes

We can write a general conservation laws in the form

$$\frac{\partial q}{\partial t}+\nabla\cdot\boldsymbol{F}(q,t)=0$$

Integrating the equations over each cell volume and using Gauss theorem to transform the divergences in Fluxes crossing the different cell boundaries::

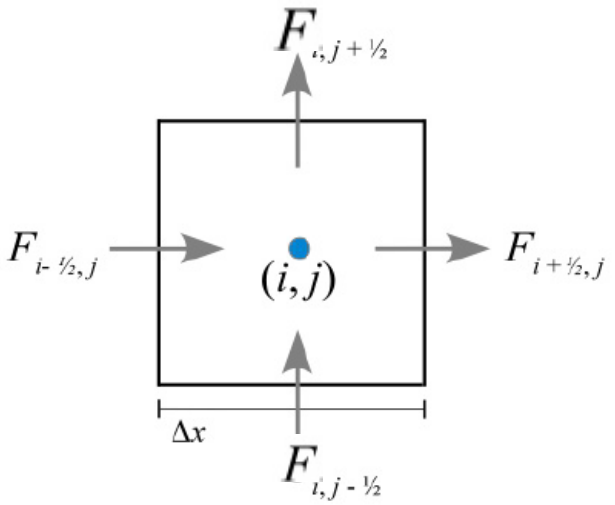

Unstructured mesh case

$$\mathbf{U}^{n+1}=\mathbf{U}^{n}-\frac{\Delta t}{V}\int\mathbf{F}\cdot\mathbf{dS}$$

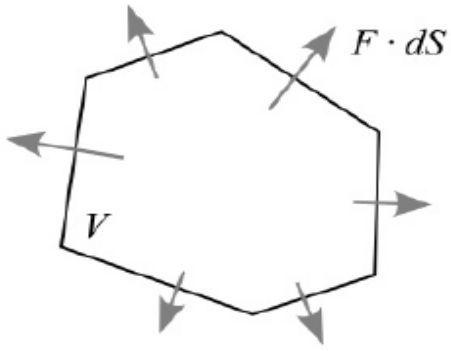

Finite Volume Schemes

We can write a general conservation laws in the form

$$\frac{\partial q}{\partial t}+\nabla\cdot\boldsymbol{F}(q,t)=0$$

Integrating the equations over each cell volume and using Gauss theorem to transform the divergences in Fluxes crossing the different cell boundaries::

Then the volume average quantiies qijk can be computed as:

$$\frac{\partial q^n_{ijk}}{\partial t}+\frac{1}{\Delta x}\left[\boldsymbol{F}^n_{i+1/2,\,jk}-\boldsymbol{F}^n_{i-1/2,\,jk}\right]+\frac{1}{\Delta y}\left[\boldsymbol{F}^n_{i,\,j+1/2,k}-\boldsymbol{F}^n_{i,\,j-1/2,k}\right]+\frac{1}{\Delta z}\left[\boldsymbol{F}^n_{i,\,j,k+1/2}-\boldsymbol{F}^n_{i,\,j,k-1/2}\right]=0$$

where q^n_{ijk} is a finite-volume quantity. The function $\boldsymbol{F}^n_{i+1/2,jk}$ is the average of $\boldsymbol{F}(q)$ over the face between cells ijk and $i+1,jk$:

$$\boldsymbol{F}^n_{i+1/2,\,jk}=\frac{1}{\Delta y\,\Delta z}\int_{y_{j-1/2}}^{y_{j+1/2}}\int_{z_{k-1/2}}^{z_{k+1/2}}\boldsymbol{F}(q,t_n)\,dy\,dz$$

We can then average over the time interval $[t_n, t_{n+1}]$ to obtain

$$q_{ijk}^{n+1} = q_{ijk}^{n} - \Delta t \left\{ \frac{1}{\Delta x}\left[\boldsymbol{F}_{i+1/2,\,jk}^{n+1/2} - \boldsymbol{F}_{i-1/2,\,jk}^{n+1/2} \right] + \frac{1}{\Delta y}\left[\boldsymbol{F}_{i,\,j+1/2,k}^{n+1/2} - \boldsymbol{F}_{i,\,j-1/2,\,k}^{n+1/2} \right] + \frac{1}{\Delta z}\left[\boldsymbol{F}_{i,\,j,\,k+1/2}^{n+1/2} - \boldsymbol{F}_{i,\,j,\,k-1/2}^{n+1/2} \right] \right\}$$

where the superscript $n+1/2$ indicates a time average.

No approximations have been introduced; if we had an exact expression for the time-averaged fluxes, we would be done. But they depend on the solution q!

In practice we must approximate the fluxes. In this process we introduce a local truncation error.

Also, if we identify the cell average of a quantity with the cell-center value of that quantity, we introduce a second-order error:

$$\frac{1}{\Delta x}\int_{x_{i-1/2}}^{x_{i+1/2}} q(x)\,dx = q(x_i) + O(\Delta x^2)$$

This is easily seen by writing $q(x)$ as a Taylor series about x_i.

Our goal is thus to obtain a *numerical flux function* that approximates $\boldsymbol{F}^{n+1/2}_{i+1/2,\,jk}$.

A simple example in 1D is the *Lax-Friedrichs method*:

$$F^{n+1/2}_{i+1/2} = \frac{1}{2}\left[F\left(q^n_i\right) + F\left(q^n_{i+1}\right)\right] - \frac{\Delta x}{2\Delta t}\left(q^n_{i+1} - q^n_i\right)$$

This results in the update step

$$q^{n+1}_i = \frac{1}{2}\left(q^n_{i-1} + q^n_{i+1}\right) - \frac{\Delta t}{2\Delta x}\left[F\left(q^n_{i+1}\right) - F\left(q^n_{i-1}\right)\right]$$

Without the second term in the flux function, this method is unconditionally unstable. The term produces an approximation to a diffusion term:

$$\frac{\partial}{\partial x}\left[\frac{\Delta x^2}{2\Delta t}\frac{\partial q}{\partial x}\right]$$

This is called *artificial viscosity*. Artificial viscosity is also used to "capture" shocks with classical numerical methods (idea due to Richtmyer and von Neumann).

Godunov's Methods

Godunov's method treats the solution as piecewise constant

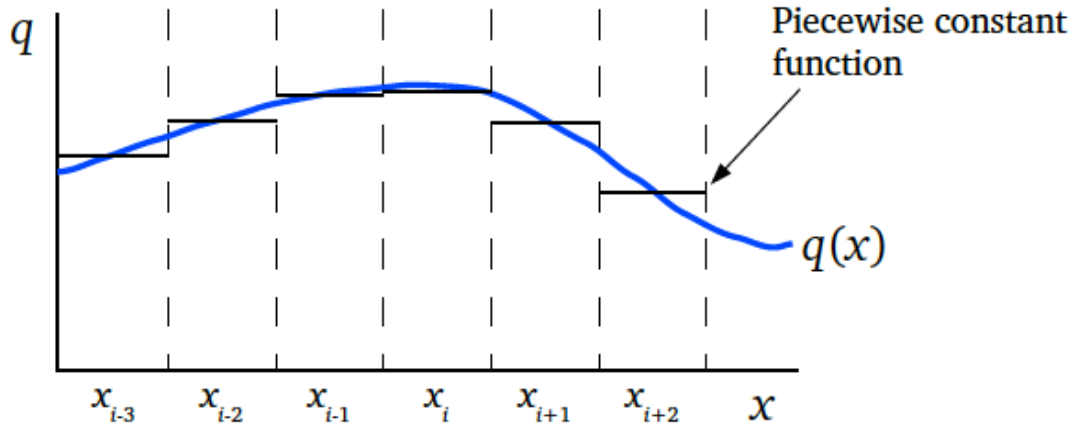

and aims to solve the time evolution over $[t_n, t_{n+1}]$ for this piecewise function *exactly*. The exact solution can then be used to produce fluxes.

The piecewise constant values are chosen to give the correct cell averages q_i.

The advantage over other methods like Lax-Friedrichs is that the solution can be nonlinear (e.g., in a shock), and we can still get accurate fluxes.

The problem of a one-dimensional initial discontinuity with constant left and right states is called the *Riemann problem*.

The Riemann Problem

The mathematician Bernhard Riemann studied the ideal gas equations in an article "Ueber die Fortpflanzung ebener Luftwellen von endlicher Schwingungsweite" published in 1860, see his Mathematical Papers.

Consider the simple linear equation

$$\frac{\partial}{\partial t}u(x,t) + c\frac{\partial}{\partial x}u(x,t) = 0\ ,$$

where c is a constant with dimensions of speed. Given an initial profile $u(x,0) = \xi(x)$, the solution of this equation is easily seen to be $u(x,t) = \xi(x - ct)$, i.e., a waveform which moves at constant speed $dx/dt = c$ without changing its shape.

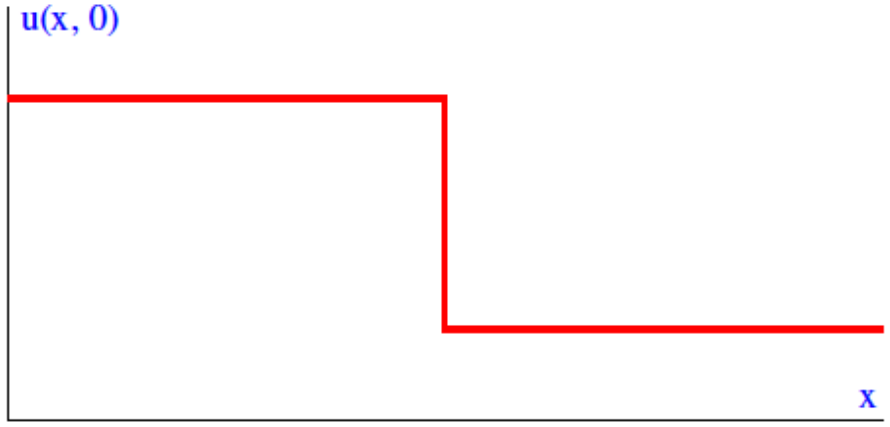

A simple form of initial condition is a step function or piece-wise constant value for $u(x,0)$, for example as shown in the figure. This type of initial condition defines a *Riemann problem*. Physically,

The Riemann Problem

this initial condition represents a *shock front* which moves with constant speed c without changing its shape.

Even though this is such a simple problem with a simple solution, it is very difficult to simulate numerically. The reason for this is that the *derivative* $\partial u/\partial x$ is infinite at the discontinuity: mathematically it is a *delta function*. Most finite difference schemes assume that the solution is smooth, i.e., the derivatives are bounded, so that a Taylor series expansion in the spatial step size h is valid. When this assumption is violated by a discontinuity, a first order scheme tends to smear out the discontinuity, and including higher orders results in unstable oscillations of the solution at the position of the discontinuity.

The Riemann Problem

- Example of a simple Riemann Problem:
- The Sod tube solution: The case when the two fluids are at rest.

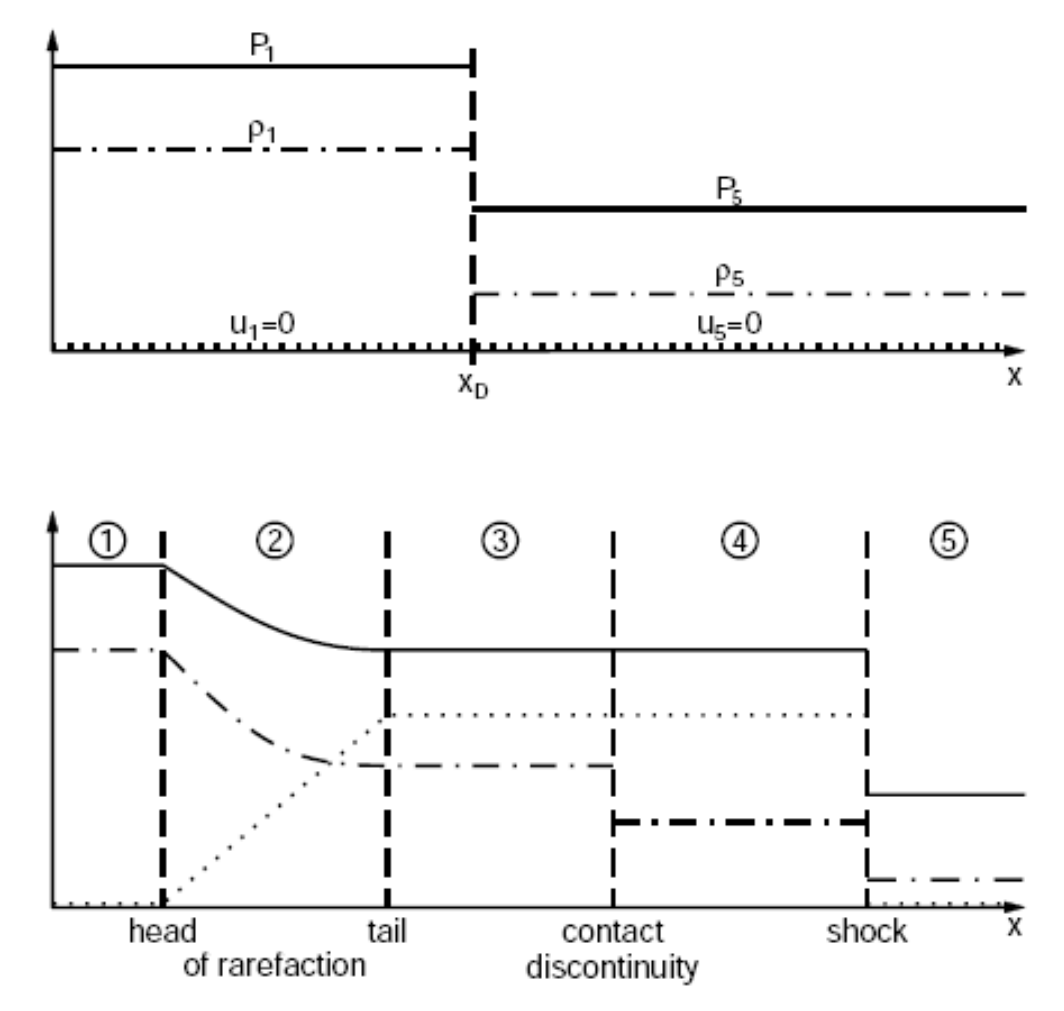

Comparison of volume average methods

$$\boldsymbol{q}_i^{n+1} = \boldsymbol{q}_i^n - \frac{\Delta t}{\Delta x}\left[\boldsymbol{F}_{i+1/2}^{n+1/2} - \boldsymbol{F}_{i-1/2}^{n+1/2}\right]$$

Godunov ($O(\Delta x, \Delta t)$)

$$\boldsymbol{F}_{i+1/2}^{n+1/2} = \boldsymbol{F}\left[\boldsymbol{q}_{i+1/2}^{n+1/2}\right]$$

$$\boldsymbol{q}_{i+1/2}^{n+1/2} = Riemann\left(\boldsymbol{q}_i^n, \boldsymbol{q}_{i+1}^n\right)(x/t = 0)$$

Lax-Friedrichs ($O(\Delta x^2, \Delta t)$)

$$\boldsymbol{F}_{i+1/2}^{n+1/2} = \frac{1}{2}\left[\boldsymbol{F}\left(\boldsymbol{q}_i^n\right) + \boldsymbol{F}\left(\boldsymbol{q}_{i+1}^n\right)\right] - \frac{\Delta x}{2\,\Delta t}\left(\boldsymbol{q}_{i+1}^n - \boldsymbol{q}_i^n\right)$$

Richtmyer (aka two-step Lax-Wendroff) ($O(\Delta x^2, \Delta t^2)$)

$$\boldsymbol{F}_{i+1/2}^{n+1/2} = \boldsymbol{F}\left(\boldsymbol{q}_{i+1/2}^{n+1/2}\right)$$

$$\boldsymbol{q}_{i+1/2}^{n+1/2} = \frac{1}{2}\left(\boldsymbol{q}_i^n + \boldsymbol{q}_{i+1}^n\right) - \frac{\Delta x}{2\,\Delta t}\left[\boldsymbol{F}\left(\boldsymbol{q}_{i+1}^n\right) - \boldsymbol{F}\left(\boldsymbol{q}_i^n\right)\right]$$

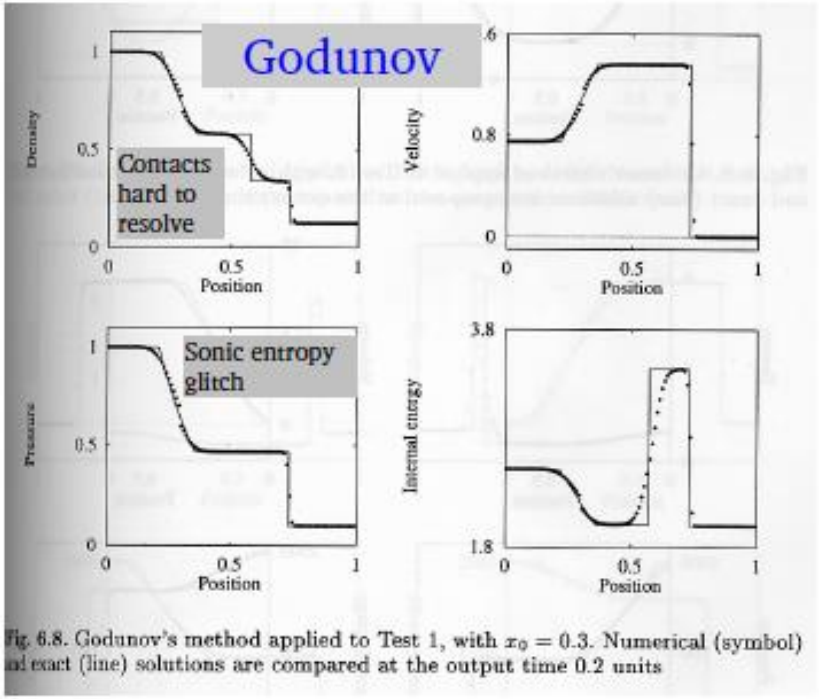

Fig. 6.8. Godunov's method applied to Test 1, with $x_0 = 0.3$. Numerical (symbol) and exact (line) solutions are compared at the output time 0.2 units

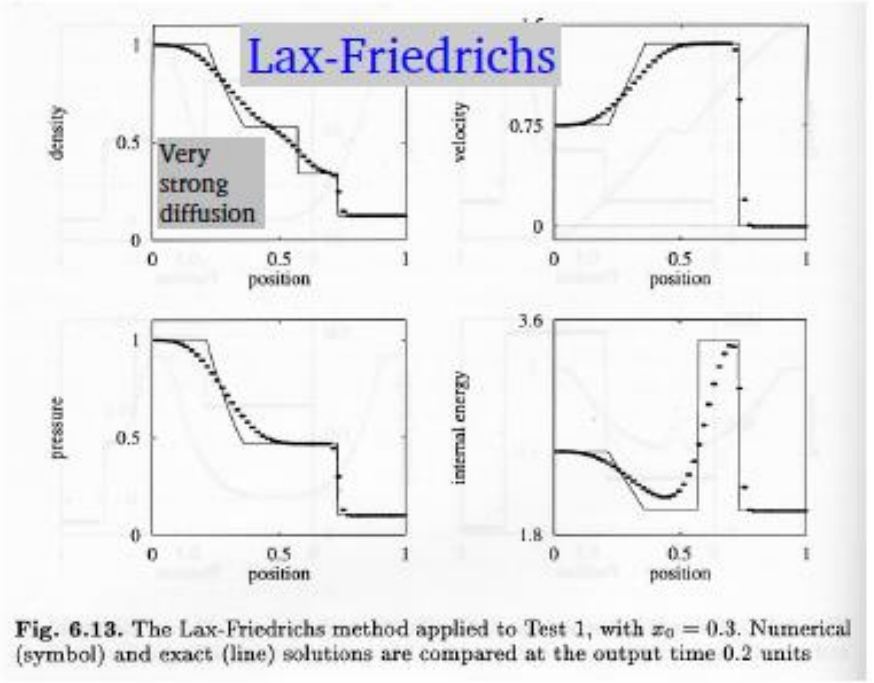

Fig. 6.13. The Lax-Friedrichs method applied to Test 1, with $x_0 = 0.3$. Numerical (symbol) and exact (line) solutions are compared at the output time 0.2 units

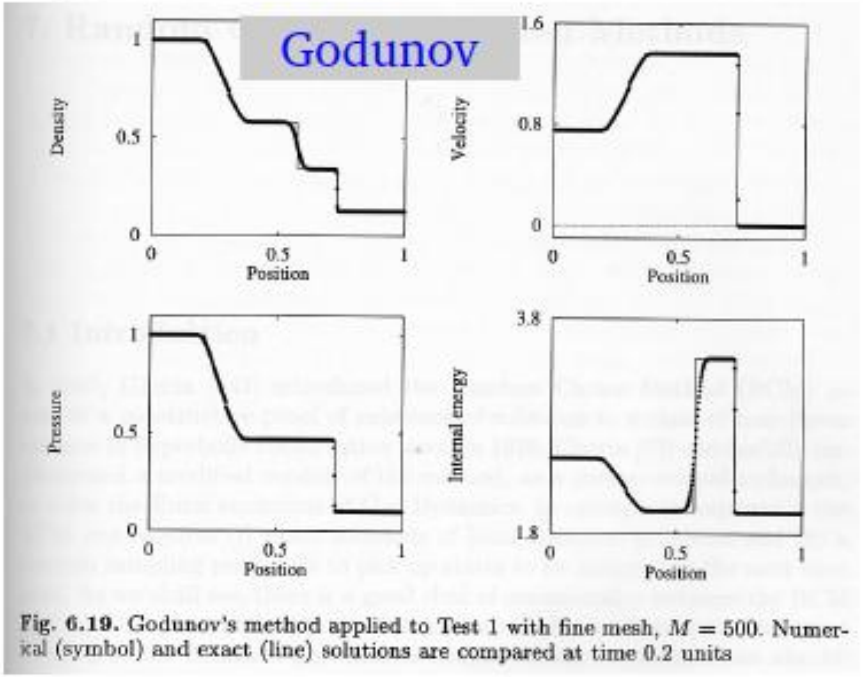

Fig. 6.19. Godunov's method applied to Test 1 with fine mesh, $M = 500$. Numerical (symbol) and exact (line) solutions are compared at time 0.2 units

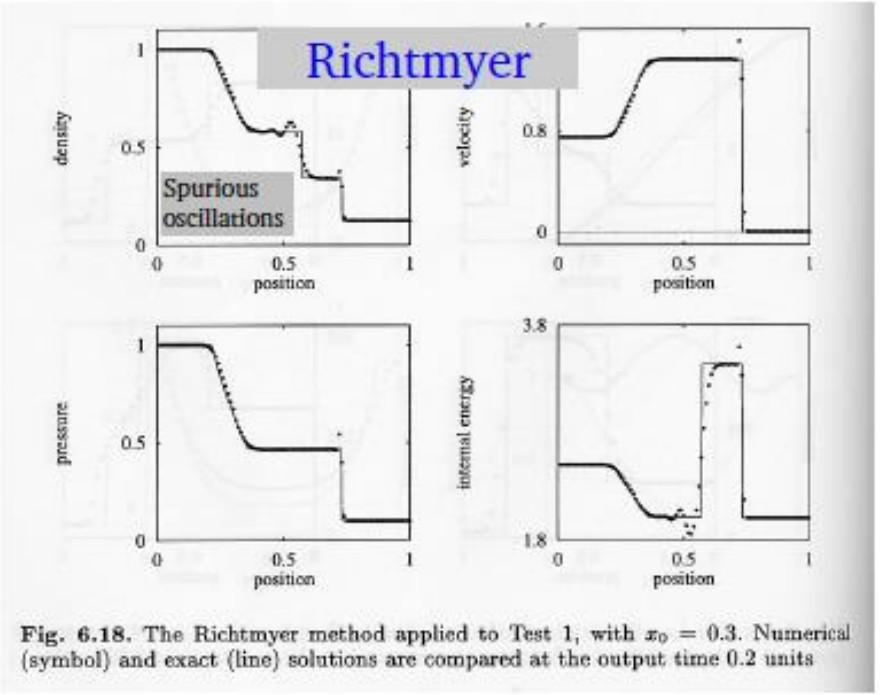

Fig. 6.18. The Richtmyer method applied to Test 1, with $x_0 = 0.3$. Numerical (symbol) and exact (line) solutions are compared at the output time 0.2 units

Higher order Godunov methods

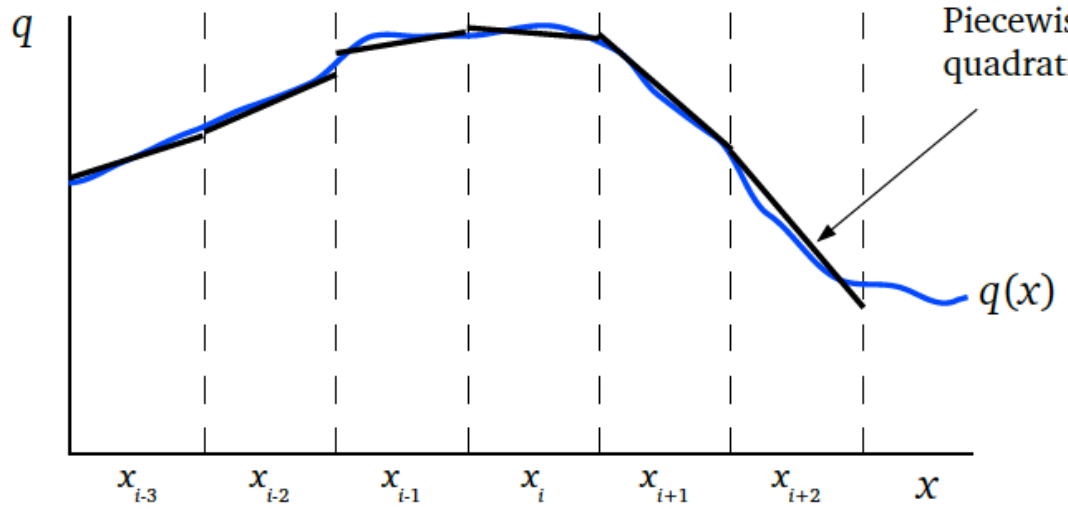

Difficulty: solving generalized Riemann problem at cell interfaces

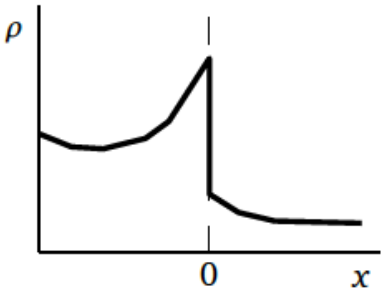

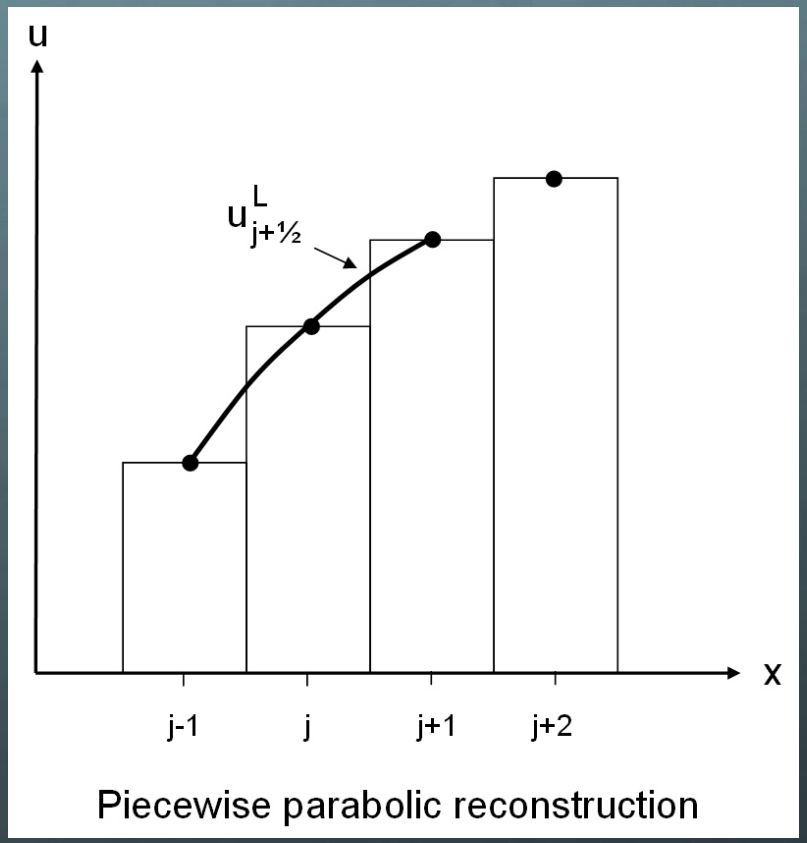

Piecewise parabolic reconstruction

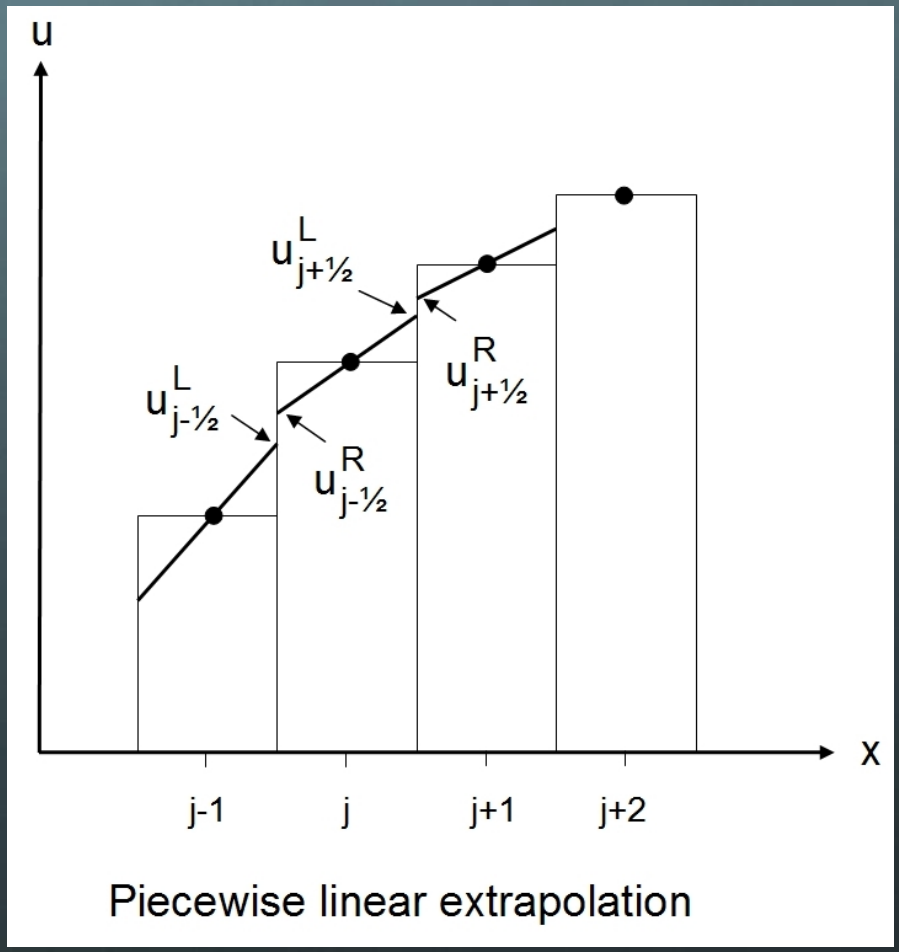

Piecewise linear extrapolation

MUSCL 1st Order linear reconstruction

MUSCL = Monotone Upwind Scheme for Conservation Laws (van Leer 1979)

Basic idea: solve ordinary Riemann problems using extrapolated L/R states to obtain *approximate* time evolution at cell boundaries

1. **Reconstruction** $\boldsymbol{q}_i^L = \boldsymbol{q}_i^n - \frac{1}{2}\boldsymbol{\sigma}_i$

$$\boldsymbol{q}_i^R = \boldsymbol{q}_i^n + \frac{1}{2}\boldsymbol{\sigma}_i$$

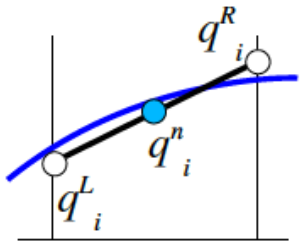

zone i

2. **Evolution** $\bar{\boldsymbol{q}}_i^L = \boldsymbol{q}_i^L + \frac{\Delta t}{2\Delta x}[\boldsymbol{F}(\boldsymbol{q}_i^L) - \boldsymbol{F}(\boldsymbol{q}_i^R)]$

$$\bar{\boldsymbol{q}}_i^R = \boldsymbol{q}_i^R + \frac{\Delta t}{2\Delta x}[\boldsymbol{F}(\boldsymbol{q}_i^L) - \boldsymbol{F}(\boldsymbol{q}_i^R)]$$

3. **Riemann problem**

$$\boldsymbol{F}_{i+1/2}^{n+1/2} = \boldsymbol{F}[\boldsymbol{q}_{i+1/2}^{n+1/2}]$$

$$\boldsymbol{q}_{i+1/2}^{n+1/2} = Riemann(\bar{\boldsymbol{q}}_i^R, \bar{\boldsymbol{q}}_{i+1}^L)(x/t = 0)$$

Order: $O(\Delta x^2, \Delta t^2)$

MUSCL

Choosing slopes for reconstruction

Interpolating polynomial:

$$q(x, t_n) \approx q_i^n + \sigma_i^n (x - x_i)$$

Constant chosen to give correct cell average in cell i (q_i)

Several choices for constraints on slope σ_i:

Centered difference (Fromm's method):

$$\sigma_i^n = \frac{q_{i+1}^n - q_{i-1}^n}{2\Delta x}$$

Upwind difference (Beam-Warming method):

$$\sigma_i^n = \frac{q_i^n - q_{i-1}^n}{2\Delta x} \quad \text{for } u^n{}_i > 0 \qquad \sigma_i^n = \frac{q_{i+1}^n - q_i^n}{2\Delta x} \quad \text{for } u^n{}_i < 0$$

Downwind difference (Lax-Wendroff method):

$$\sigma_i^n = \frac{q_{i+1}^n - q_i^n}{2\Delta x} \quad \text{for } u^n{}_i < 0 \qquad \sigma_i^n = \frac{q_i^n - q_{i-1}^n}{2\Delta x} \quad \text{for } u^n{}_i > 0$$

Slope limiters

As long as $\frac{1}{\Delta x}\int_{x_{i-1/2}}^{x_{i+1/2}} q(x,t_n)\,dx = q_i^n$ for our polynomials, slopes can be whatever we need

Notice that at discontinuities, divided differences give meaningless slopes:

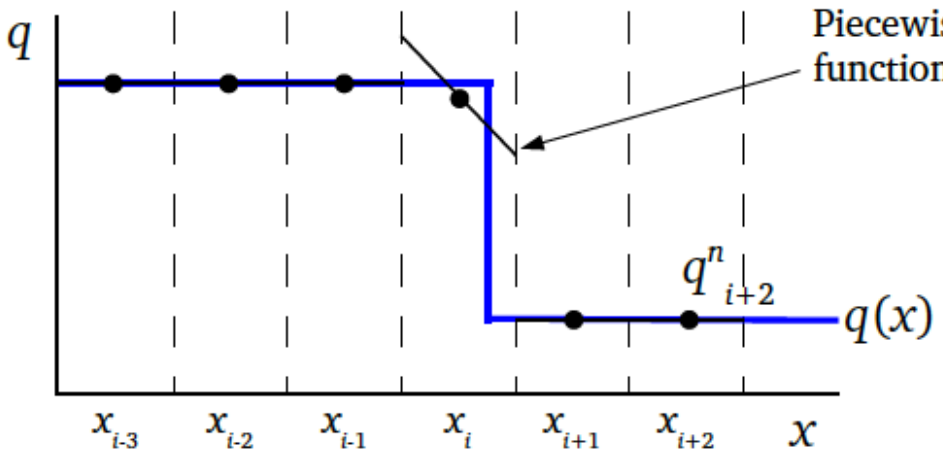

Unless we "flatten" the interpolating polynomial at discontinuities, we will introduce oscillations at these locations.

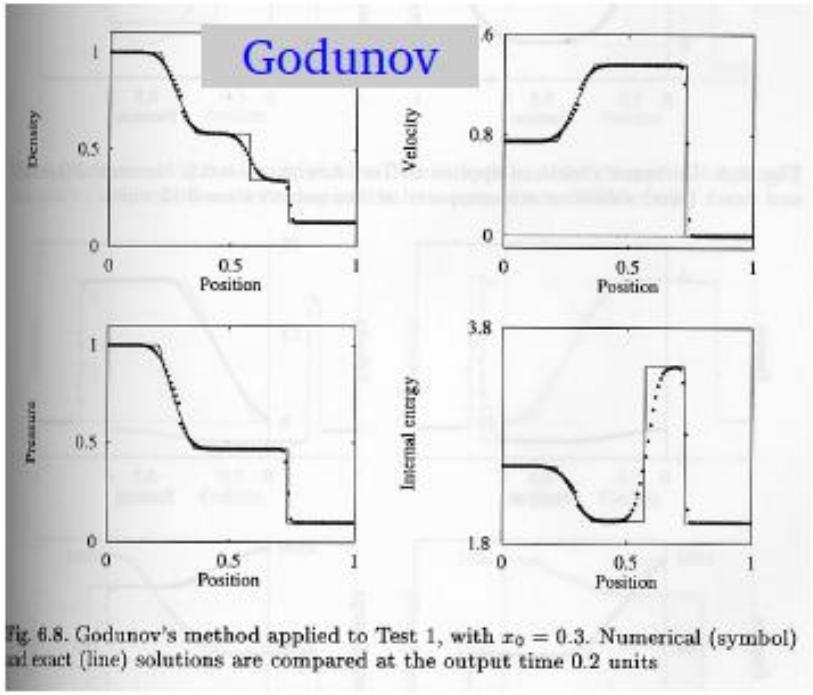

Fig. 6.8. Godunov's method applied to Test 1, with $x_0 = 0.3$. Numerical (symbol) and exact (line) solutions are compared at the output time 0.2 units

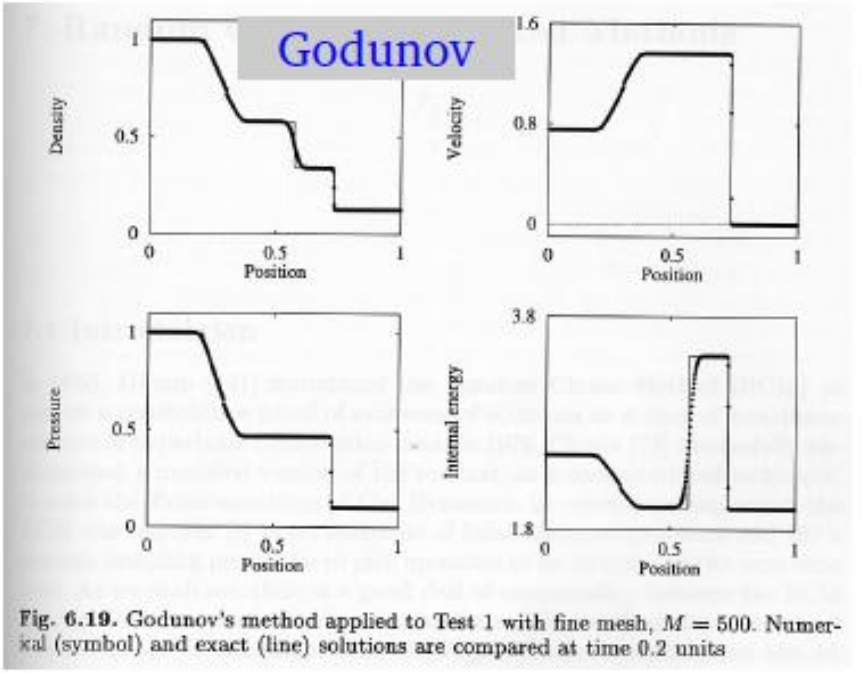

Fig. 6.19. Godunov's method applied to Test 1 with fine mesh, $M = 500$. Numerical (symbol) and exact (line) solutions are compared at time 0.2 units

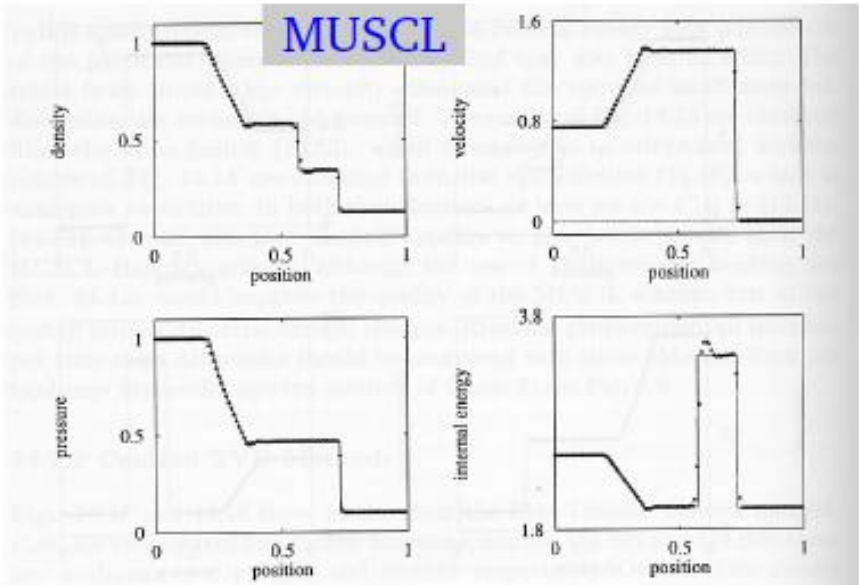

Fig. 14.11. MUSCL–Hancock scheme, HLLC Riemann solver and SUPERBEE for to Test 1. Numerical (symbol) and exact (line) solutions at time 0.2 units

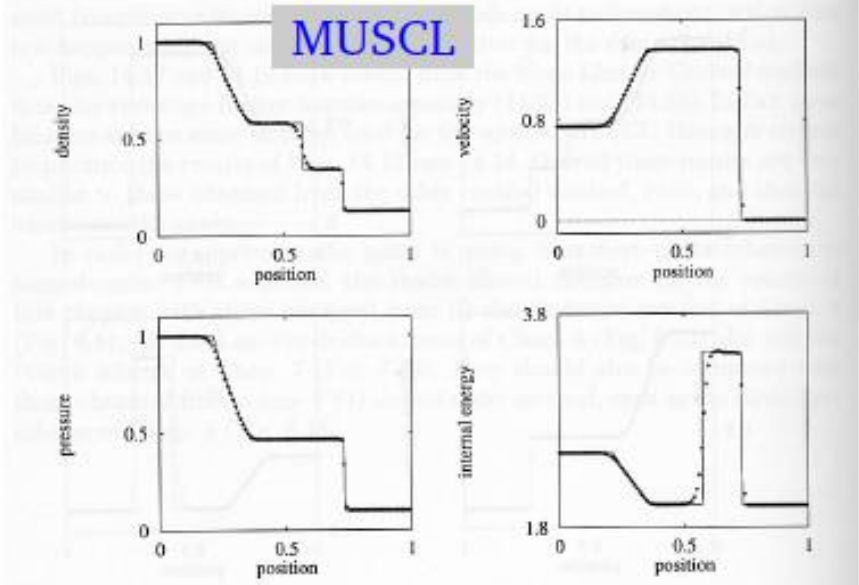

Fig. 14.12. MUSCL–Hancock Scheme with HLLC Riemann solver and MINBEE applied to Test 1. Numerical (symbol) and exact (line) solutions at time 0.2 units

No characteristic decomposition applied to slope limiter

PPM: 2nd order interpolation

Use quadratic interpolating polynomials in MUSCL-type scheme ($O(\Delta t^2)$)

$$q(\xi) \approx q_L + \xi[\delta q + q_6(1-\xi)], \qquad \xi \equiv \frac{x - x_{i-1/2}}{\Delta x} = 0 \ldots 1$$

In principle should yield $O(\Delta x^3)$ accuracy, but this was found to be cost-ineffective; some parts of algorithm limit method to $O(\Delta x^2)$ overall

Interpolation is actually performed on $\int q(x)dx$ using a *cubic* polynomial, which is then differentiated (to get $O(\Delta x^2)$ even on nonuniform meshes)

$$q_{R,i} = \frac{1}{12}\left[-q^n_{i+2} + 7\,q^n_{i+1} + 7\,q^n_i - q^n_{i-1}\right]$$

$$\delta q_i = \frac{1}{2}\left[q^n_{i+1} - q^n_{i-1}\right] = q_{R,i} - q_{L,i}$$

$$q_{6,i} = 6\left[q^n_i - \frac{1}{2}(q_{L,i} + q_{R,i})\right]$$

The linear slope δq_i is limited using the monotonized central-difference limiter.

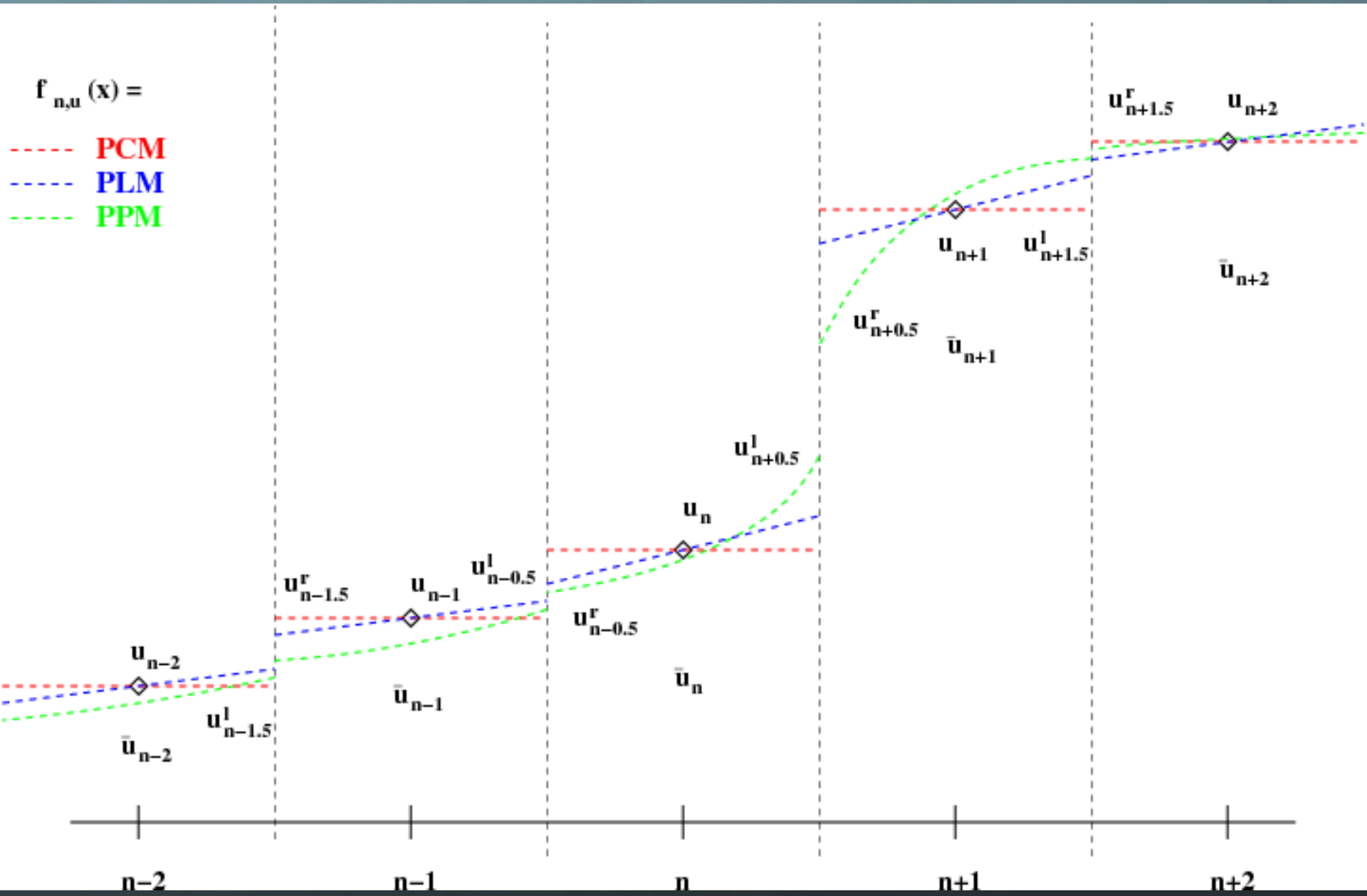
f n,u (x) =
PCM
PLM
PPM
u r n+1.5
u n+2
u n+1
u l n+1.5
ū n+2
u r n+0.5
ū n+1
u l n+0.5
u n
u r n−1.5
u n−1
u l n−0.5
u r n−0.5
u n−2
ū n−1
ū n
u l n−1.5
ū n−2
n−2
n−1
n
n+1
n+2

Approximate Riemann Solvers

- The Riemann problem has a solution that can be obtained using Rankine-Hugoniot conditions at the interfaces (conservation properties). But it is not very useful for numerical problems because it involves solving algebraic equations.

- Approximate Riemann solvers have been proposed as a efficient way to estimate the fluxes across the cell interfaces.

Two-shock Riemann solver

Treat rarefactions as "entropy-reducing shocks"
Benefit: no expensive fractional powers
Drawback: incorrect entropy behavior in rarefactions

Harten-Lax-van Leer (HLL) Riemann solver

Treat solution as consisting of two waves separated by three constant states.
Benefit: direct solution, no iteration required
Drawback: poor treatment of contact discontinuities

Roe Riemann solver

Solve Riemann problem for linearized Euler equations
Benefit: straightforward to adapt to new systems of equations
Drawback: entropy glitch, problems in rarefaction fans

Roe Solver

Consider again the Riemann problem

$$\begin{aligned} \mathbf{q}_t + \mathbf{f}(\mathbf{q})_x &= 0\,, \\ \mathbf{q}(x,0) &= \begin{cases} \mathbf{q}_l & \text{if} \quad x < 0\,, \\ \mathbf{q}_r & \text{if} \quad x > 0\,, \end{cases} \end{aligned}$$

where for the x-split three-dimensional Euler equation

$$\mathbf{q} = \begin{pmatrix} \rho \\ \rho u \\ \rho v \\ \rho w \\ E \end{pmatrix}, \qquad \mathbf{f}(\mathbf{q}) = \begin{pmatrix} \rho u \\ \rho u^2 + p \\ \rho uv \\ \rho uw \\ u(E+p) \end{pmatrix}.$$

Roe Solver

Using the chain rule, the conservation law

$$\mathbf{q}_t + \mathbf{f}(\mathbf{q})_x = 0$$

may be written as

$$\mathbf{q}_t + \mathbf{A}(\mathbf{q})\mathbf{q}_x = 0\,, \qquad \mathbf{A}(\mathbf{q}) = \frac{\partial \mathbf{f}}{\partial \mathbf{q}}\,.$$

Roe's approach consists in replacing the Jacobian matrix $\mathbf{A}(\mathbf{q})$ by a *constant Jacobian*

$$\tilde{\mathbf{A}} = \tilde{\mathbf{A}}(\mathbf{q}_l, \mathbf{q}_r)$$

resulting in the Riemann problem for the *linear system*

$$\begin{aligned} \mathbf{q}_t + \tilde{\mathbf{A}}\mathbf{q}_x &= 0\,, \\ \mathbf{q}(x,0) &= \begin{cases} \mathbf{q}_l & \text{if} \quad x < 0\,, \\ \mathbf{q}_r & \text{if} \quad x > 0\,, \end{cases} \end{aligned}$$

which can be solved exactly.

ADAPTIVE MESH EULERIAN METHODS

INCREASE THE DYNAMICAL RANGE OF EULERIAN METHODS

- Achieving high local resolution in space, time and mass imply decreasing the mesh size. For astrophysical problems this is almost impossible to achieve:
  - For Galaxy formation, typical resolution is around 10pc and the minimum volume to form a galaxy is around 10Mpc. With equal mesh size, the number of cells $> 10^{18}$!!
  - But most of the original volume is not needed to be resolved with this resolution.
- Some kind of adaptivness is needed for eulerian methods to be competitive against SPH.

INCREASE THE DYNAMICAL RANGE OF EULERIAN METHODS

- Two kind of strategies can be used to increase the dynamical range of Eulerian hydrodynamics:

  - Adaptive Mesh Refinement
  - Moving Mesh techniques.

AMR

- Add new staggered meshes in regions of high density

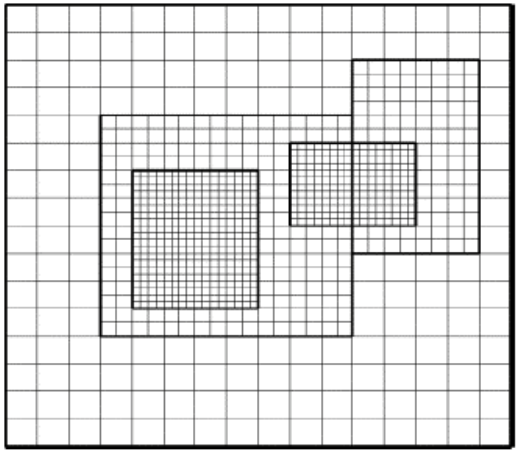

patch-based
refinement strategy
(e.g ENZO)

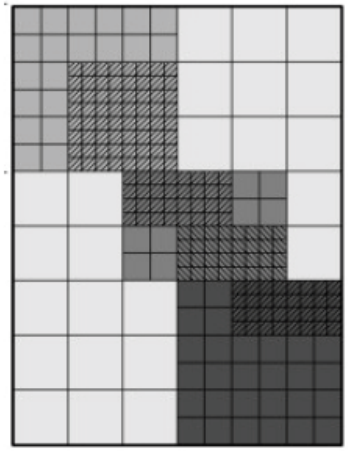

tree-based
refinement strategy
(e.g RAMSES)

AMR

AMR:

- Use a hierarchy of nested grids that allows in principle arbitrary dynamic range. Refinement criteria can be chosen almost arbitrarily.
- Quick motion of a small high-resolution region requires however frequent changes of the mesh hierarchy.
- Accuracy at grid boundaries suffers and normally goes down to 1st order.

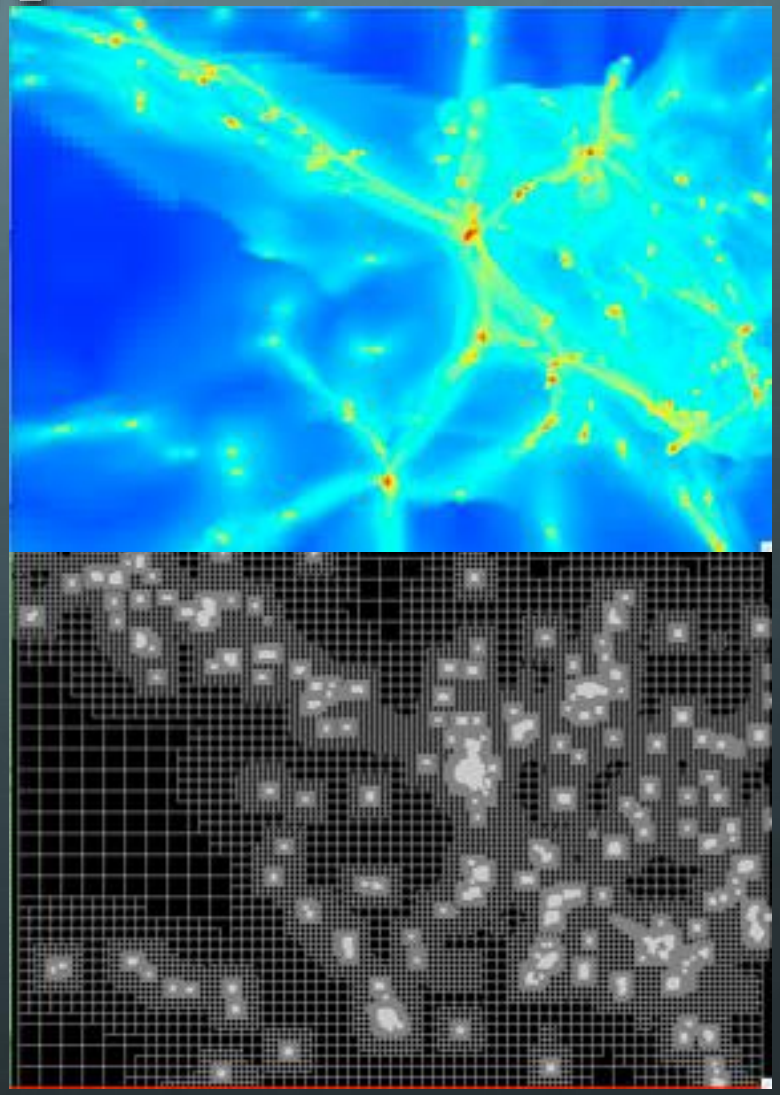

AMR CODES IN ASTROPHYSICS

ENZO: Greg Bryan, Michael Norman…

ART: Andrey Kravtsov, Anatoly Klypin

RAMSES: Romain Teyssier

NIRVANA: Udo Ziegler

AMRVAC: Gabor Thot and Rony Keppens

FLASH: The Flash group (PARAMESH lib)

ORION: Richard Klein, Chris McKee, Phil Colella

PLUTO: Andrea Mignone (CHOMBO lib, Phil Colella)

CHARM: Francesco Miniati (CHOMBO lib, Phil Colella)

ASTROBear: Adam Frank…

- http://www.astrosim.net

MOVING MESH METHODS

MOVING-MESH hydrodynamics

- Use also eulerian methods to solve fluid equations on a mesh.
- The mesh is adapting to the fluid structures:
  - Deforming the cells while keeping same number of cell elements .
  - Using unstructured meshes.

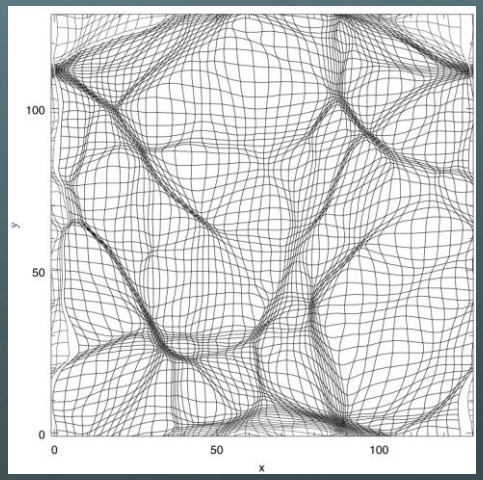

MMH-code, Pen, 1995, ApJS,115,19

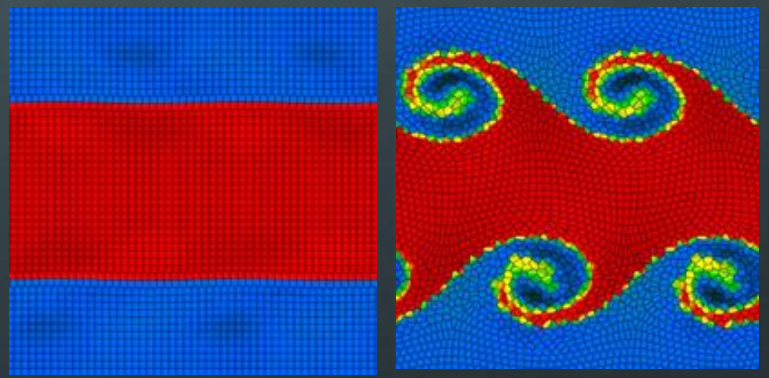

Arepo,
Springel, MNRAS, 401,791, 2010

AREPO

- Use Voronoi tesselation algorithm to generate the mesh:

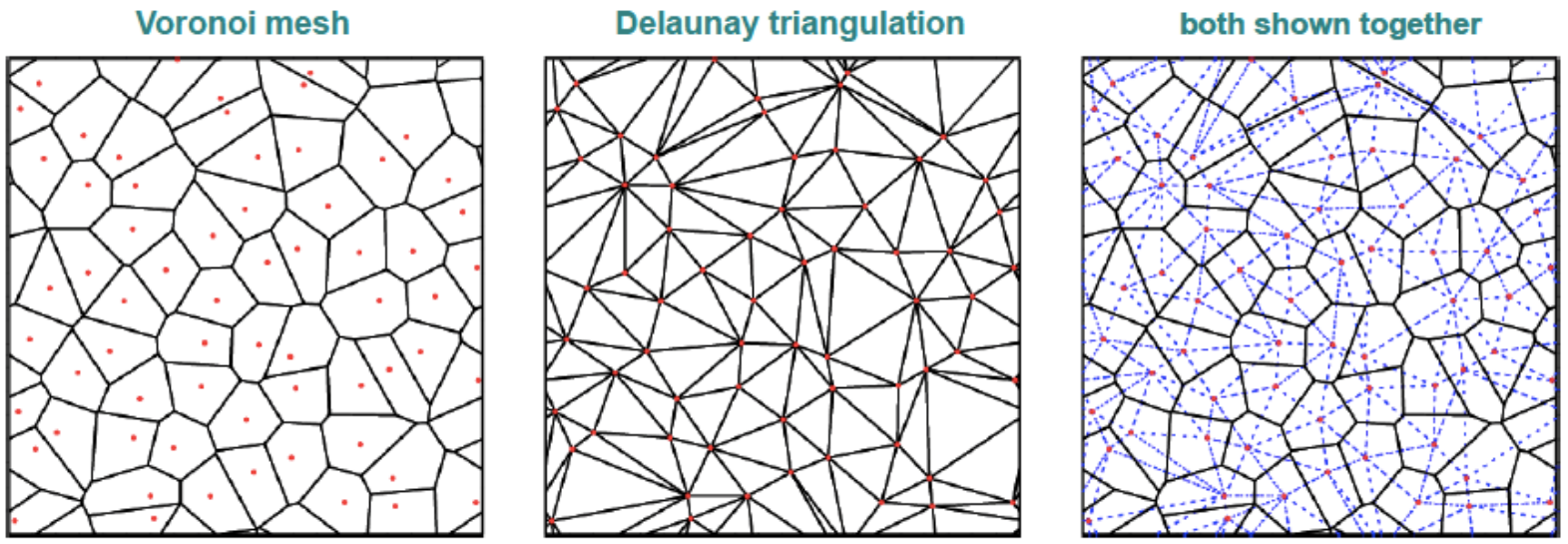

- Each Voronoi cell contains the **space closest** to its generating point
- The Delaunay triangulation contains only triangles with an **empty circumcircle**. The Delaunay tiangulation maximizes the minimum angle occurring among all triangles.
- The centres of the circumcircles of the Delaunay triangles are the vertices of the Voronoi mesh. In fact, the two tessellations are the topological **dual graph** to each other.

AREPO

The fluxes are calculated with an exact Riemann solver in the frame of moving cell boundary

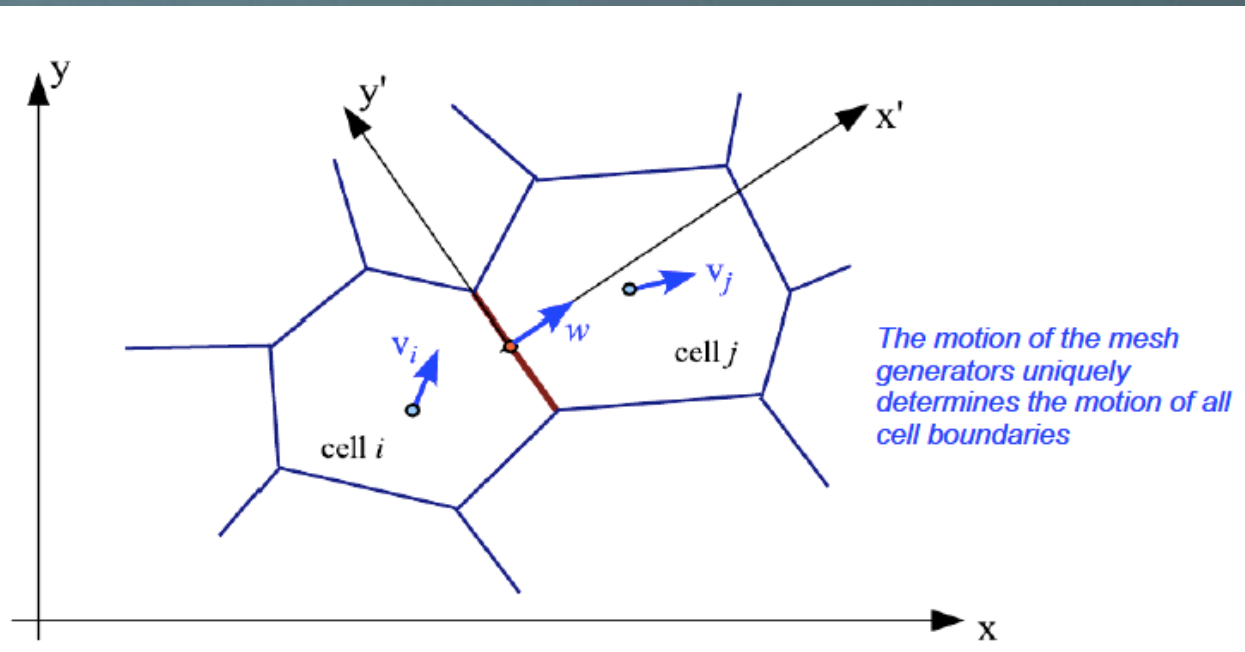

AREPO

- KH test

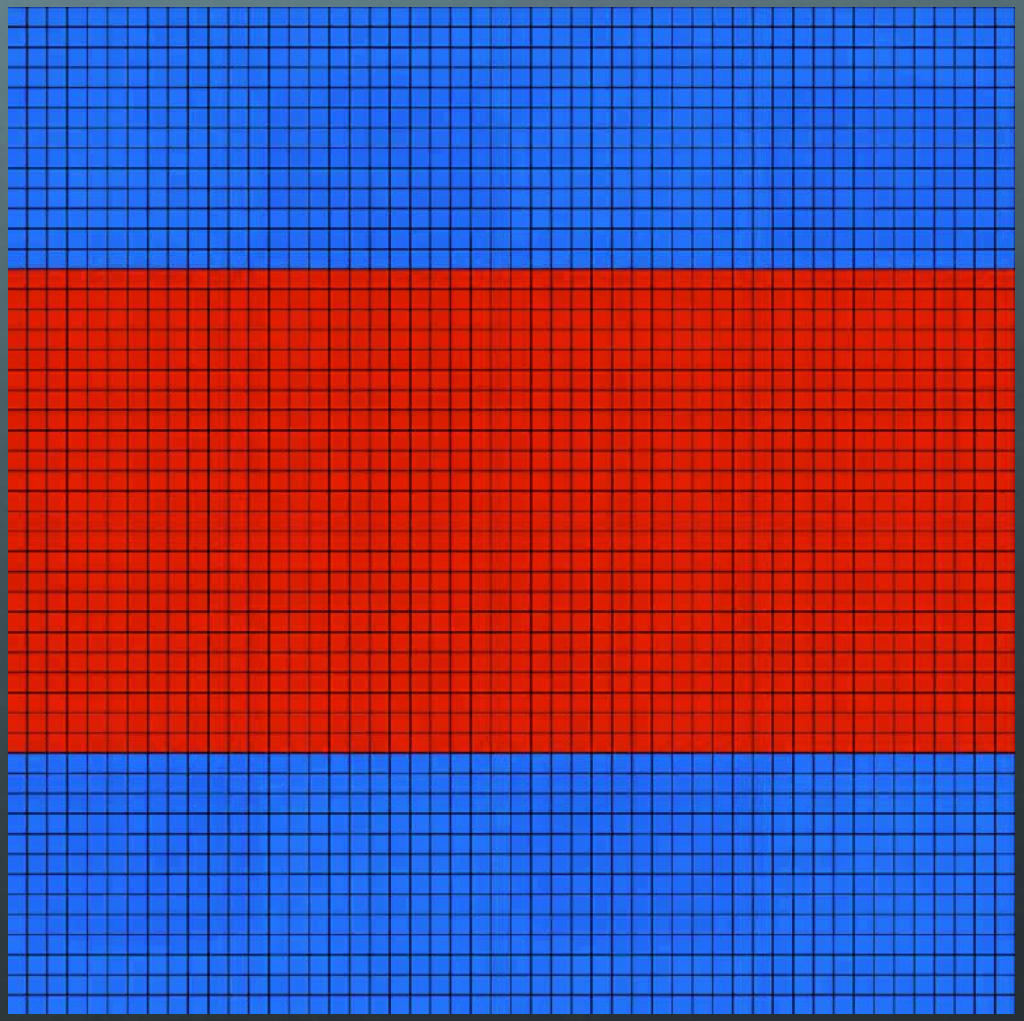

AREPO

- Sedov Blast

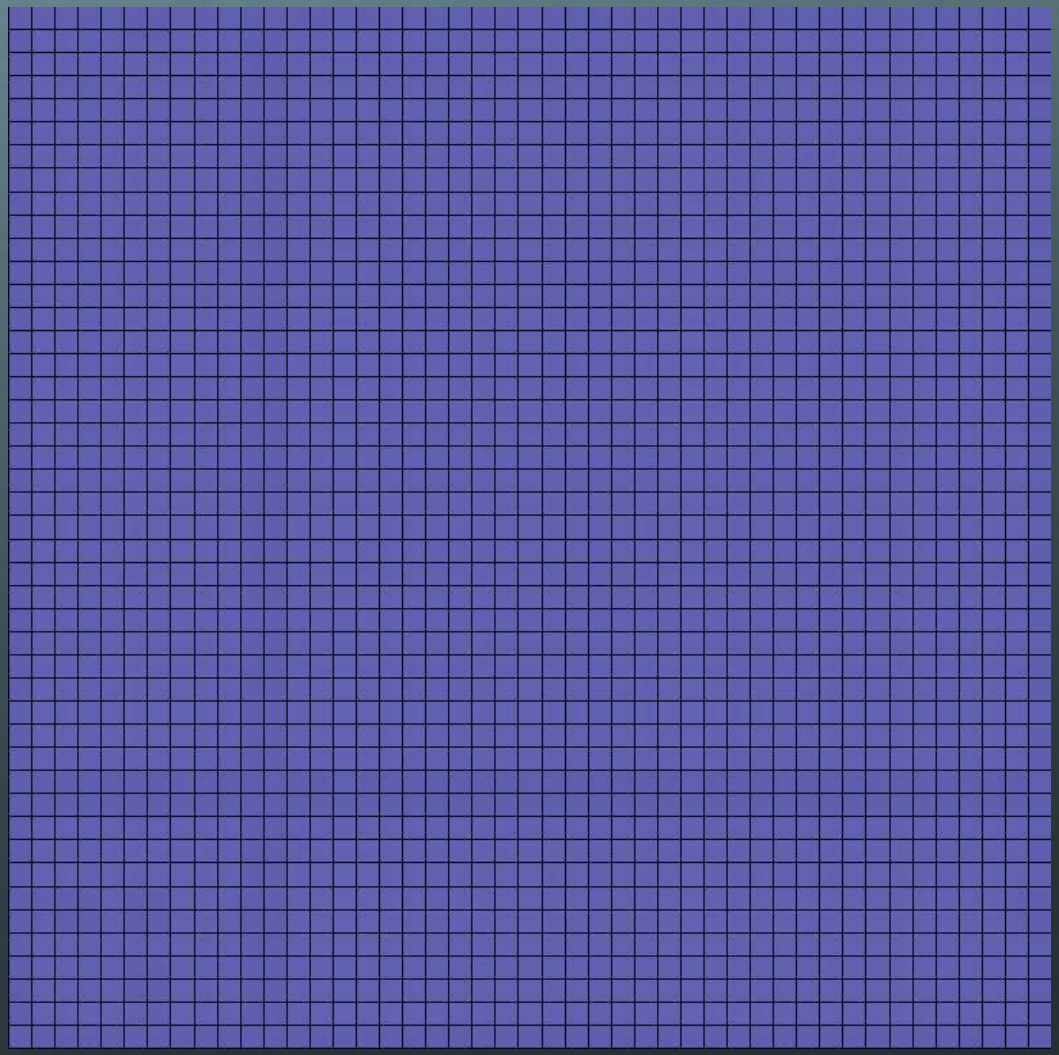

AREPO

GAS BLOBS AROUND GALAXY SIMULATION

Wadepul & Springel 2011

AREPO

GADGET

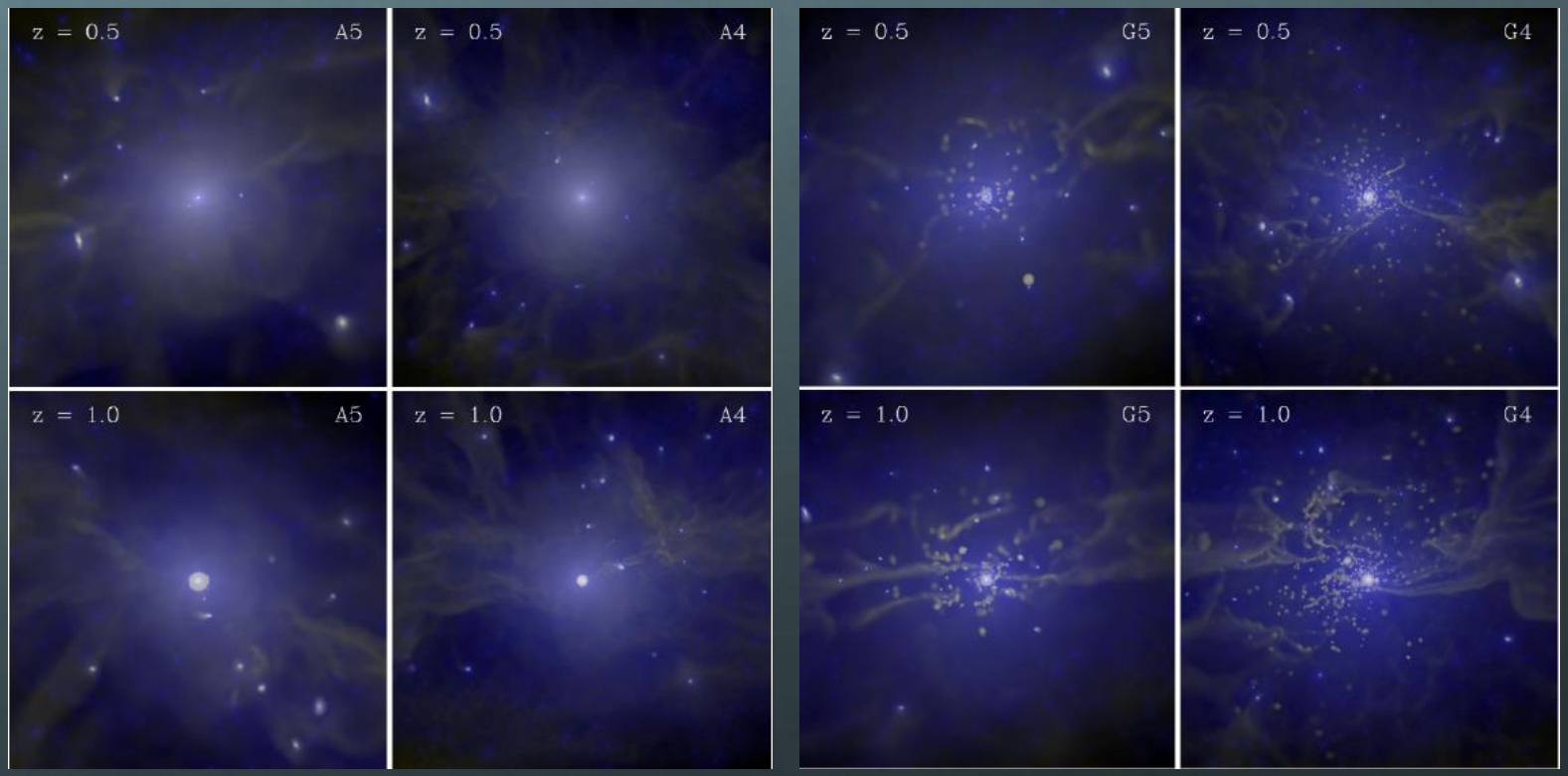

Baryonic processes

- Baryonic matter is subject to many different processes due to electromagnetic and strong interactions:
  - Radiative atomic cooling and UV heating.
  - Gravothermal catastrophies
  - Star and Black hole formation
  - Feedbacks: thermal injection by exploding stars and metal enrichments.
- Much smaller scales than we can resolve gravity and hydro forces (< pc)

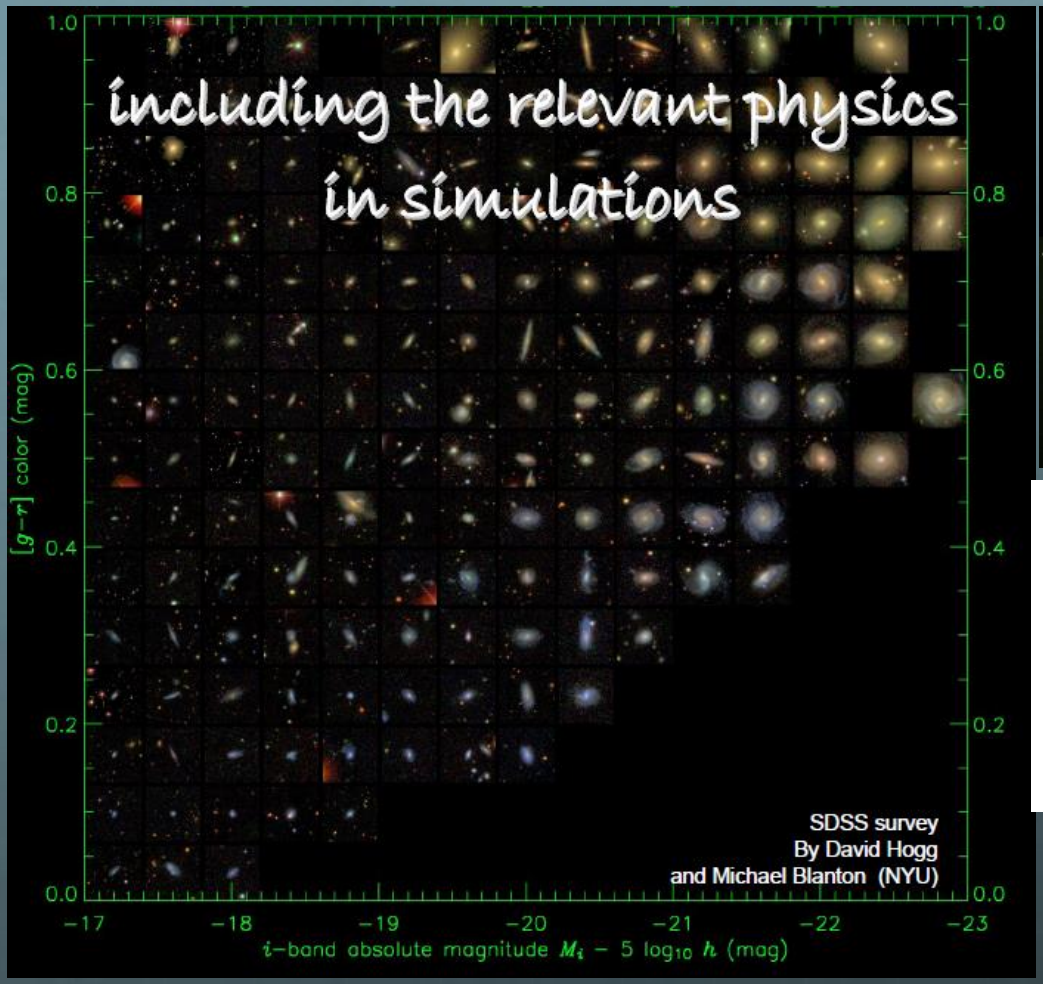

gas cooling rates for primordial gas composition

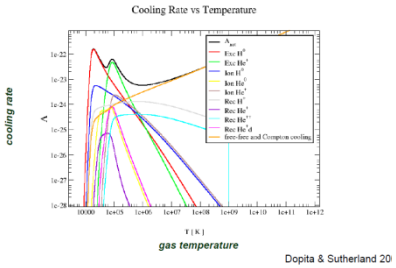

Dopita & Sutherland 20

dependence of cooling rate on metallicity

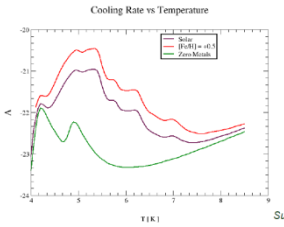

Sutherland & Dopita 1993, ApJS

Given the rates, how is cooling included in the simulations?

$$\frac{\partial \rho}{\partial t} + \nabla \rho \mathbf{u} = 0,$$

$$\frac{\partial \mathbf{u}}{\partial t} + (\mathbf{u} \cdot \nabla)\mathbf{u} = -\nabla \Phi - \frac{\nabla P}{\rho},$$

$$\frac{\partial E}{\partial t} + \nabla \cdot [(E + P)\mathbf{u}] = -\rho \mathbf{u} \cdot \nabla \Phi + (\Gamma - \mathrm{L}),$$

$$\nabla^2 \Phi = 4\pi G(\rho_{tot} + 3P_{tot}/c^2) - \Lambda,$$

$$\varepsilon = \frac{1}{\gamma - 1}\frac{P}{\rho},$$

- net cooling/heating modify the internal energy of the gas and hence the total energy $E=v^2/2+\varepsilon$
- so cooling/heating is included as sink/source term on r.h.s. of the energy equation
- the only subtlety is that the rate of energy change (e.g., cooling time) can be much shorter than local dynamical time which sets the integration step of the hydro equations

starformation in simulations

HST image of the Antennae galaxies

Once a stellar particle is formed it is assigned mass, time of birth, metallicity of the parent cell, etc. These properties allow then to model spectra of galaxies and to calculate its optical properties (luminosity, colors,…)

starformation can be assume to occur over some time, rather than instantly

$$\Delta m_{\rm SF} = m_*(\Delta t/t_{\rm dyn})[(t-t_*)/t_{\rm dyn}]\,\exp\,[-(t-t_*)/t_{\rm dyn}]$$

which allows to spread heating due stellar feedback over time

$$\Delta E_{\rm SN}/\Delta t = (\Delta m_{\rm SF}/\Delta t)c^2\epsilon_{\rm SN}$$
$$\Delta E_{\rm v}/\Delta t = (\Delta m_{\rm SF}/\Delta t)c^2\epsilon_{\rm UV}\,g_{\rm v}$$

$$\epsilon_{\rm SN} = 10^{-4.5} \qquad \epsilon_{\rm UV} = 10^{-4.0}$$

star formation in nutshell

convert gas mass into collisionless stellar particles in cold, dense regions according to rate:

$$\dot{\rho}_* = C_*\left(\frac{\rho_{\rm gas}}{\rho_0}\right)^{\alpha}, \quad T < T_*, \quad \rho_{\rm gas} > \rho_*$$

sometimes compression condition is enforced to form stellar particles only in the regions of converging flow

$$\nabla\cdot\boldsymbol{v} < 0$$

normalization C is chosen so that the empirical Kennicutt's star formation law is reproduced:*

$$\Sigma_{\rm SFR} = (2.5\pm0.7)\times10^{-4}\left(\frac{\Sigma_{\rm gas}}{1\ {\rm M_\odot pc^{-2}}}\right)^{1.4\pm0.15}\ {\rm M_\odot yr^{-1}kpc^{-2}}$$

Tag all mesh cells (or gas particles in an SPH simulation) for which the following set of conditions is satisfied:

$$\nabla\cdot\boldsymbol{v} < 0 \Rightarrow \text{contracting},$$

$$t_{\rm cool} < t_{\rm dyn} \equiv \sqrt{\frac{3\pi}{32G\rho_{\rm tot}}} \Rightarrow \text{cooling rapidly}$$

$$m_b > m_{\rm J} \quad \Rightarrow \text{gravity unstable}$$

Take mass from the gas mass of the cell and convert it into a stellar particle:

$$\Delta m_b = -m_b\,\Delta t/t_{\rm dyn} \quad \text{and} \quad m_* = +m_b\,\Delta t/t_{\rm dyn}$$

Stellar particles are assigned the momentum and position of their parent cell (or gas particle). Subsequently, they are followed as collisionless particles along with DM particles using standard N-body techniques.

Sources and Sink terms due to radiative processes

- Conservation equations can be modified to account for sources and sink terms of mass, momentum and energy:

$$\frac{\partial \mathbf{U}}{\partial t} + \nabla \cdot \mathbf{F}(\mathbf{U}) = \sum_i S_i(\mathbf{U})$$

Right hand-side may describe physics such as radiative cooling, diffusion or chemistry.

- Time Operator splitting:
  - First solve the hydro steps (subject to CFL condition)
  - Between hydro timesteps, solve the equations to account for the r.h.s terms

This means we can split off the extra physics:

$$\frac{\partial \mathbf{U}}{\partial t} + \nabla \cdot \mathbf{F}(\mathbf{U}) = S_{\rm chem}(\mathbf{U})$$

α:
$$\frac{\partial \mathbf{U}}{\partial t} + \nabla \cdot \mathbf{F}(\mathbf{U}) = 0$$

β:
$$\frac{\partial \mathbf{U}}{\partial t} = S_{\rm chem}(\mathbf{U})$$

2016

AREPO CODE

75/h Mpc box.
~10^10 computational elements (particles, mesh, tracers)
Physics models:

- Gas cooling and photo-ionization
- Star formation and ISM model
- Stellar evolution
- Stellar feedback
- Black holes and SMBH feedback

http://www.illustris-project.org/

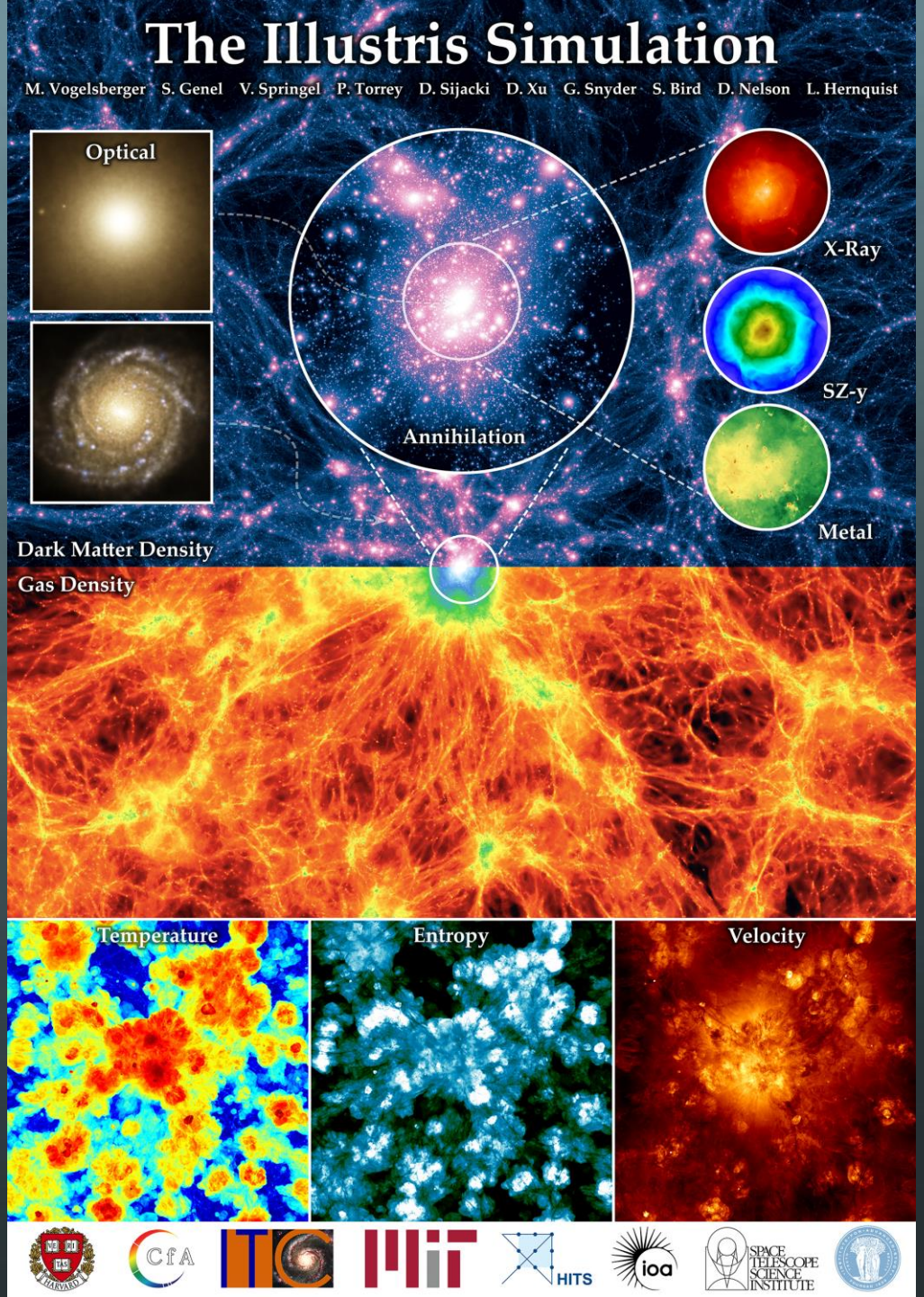

Other physical process

- Besides the long range forces acting on the different components of the Universe: (gravity and pressure) there are some situations in Astrophysics in which the fluid is also subject to other interactions:
  - *Magnetic fields in ionized plasmas*
  - *Ionizing radiation field from stellar sources*
  - *Presence of strong gravitational fields*
  - *Gas outflows at relativistic speeds.*

Other physical process

- Magento-Hydrodynamics (MHD) hyperbolic equations:

$$\frac{\partial \rho}{\partial t} + \nabla \cdot (\rho \mathbf{u}) = 0,$$

$$\frac{\partial \rho \mathbf{u}}{\partial t} + \nabla \cdot (\rho \mathbf{u} \otimes \mathbf{u} - \mathbf{B} \otimes \mathbf{B} + P_{\text{tot}} \mathbb{I}) = 0,$$

$$\frac{\partial E_{\text{tot}}}{\partial t} + \nabla \cdot [\mathbf{u}(E_{\text{tot}} + P_{\text{tot}}) - \mathbf{B}\,(\mathbf{B} \cdot \mathbf{u})] = 0,$$

$$E_{\text{tot}} = \rho\epsilon + \frac{1}{2}\rho \mathbf{u} \cdot \mathbf{u} + \frac{1}{2}\mathbf{B} \cdot \mathbf{B},$$

$$P_{\text{tot}} = P(\rho, \epsilon) + \frac{1}{2}\mathbf{B} \cdot \mathbf{B}.$$

- Godunov methods can be used to solve them on finite volumes, including B as additional fluid state.
  - (see Teyssier ANRAA review)

Other physical processes

- **THE RADIATION TRANSPORT EQUATION:**

Conservation of photons in phase-space

$$\frac{1}{c}\frac{\partial I_\nu}{\partial t} + \mathbf{n}\cdot\nabla I_\nu = -\kappa_\nu I_\nu + \eta_\nu$$

$I_\nu(\mathbf{x},\mathbf{n},t)$ radiation specific intensity

$\kappa_\nu(\mathbf{x},\mathbf{n},t)$ absorption coefficient

$\eta_\nu(\mathbf{x},\mathbf{n},t)$ source function

Source terms: microscopic collisions leading to absorption and emission.

Moments of the radiation transfer equation

Radiation energy:

$$E_\nu(\mathbf{x},t) = \int I_\nu(\mathbf{x},\mathbf{n},t)\frac{\mathrm{d}\Omega}{c}$$

Radiation flux:

$$\mathbf{F}_\nu(\mathbf{x},t) = \int I_\nu(\mathbf{x},\mathbf{n},t)\mathbf{n}\frac{\mathrm{d}\Omega}{c}$$

Pressure tensor:

$$\mathbb{P}_\nu(\mathbf{x},t) = \int I_\nu(\mathbf{x},\mathbf{n},t)\mathbf{n}\otimes\mathbf{n}\frac{\mathrm{d}\Omega}{c}$$

Energy equation:

$$\frac{\partial E_\nu}{\partial t} + \nabla\cdot\mathbf{F}_\nu = -\kappa_\nu c E_\nu + S_\nu$$

Flux equation:

$$\frac{\partial \mathbf{F}_\nu}{\partial t} + c^2\nabla\cdot\mathbb{P}_\nu = -\kappa_\nu c\mathbf{F}_\nu$$

Other physical processes

- **Radiation Hydrodynamics:**

Fluid energy equation writes: $\frac{\partial E}{\partial t} + \nabla \cdot \mathbf{u}(E + P) = \Gamma - \Lambda$

Heating and cooling functions: $\Gamma = \int \kappa_\nu c E_\nu \mathrm{d}\nu \qquad \Lambda = \int S_\nu \mathrm{d}\nu$

Momentum equation writes: $\frac{\partial \rho \mathbf{u}}{\partial t} + \nabla \cdot (\rho \mathbf{u} \otimes \mathbf{u} + P\mathbb{I}) = -\rho \nabla \phi + \mathbf{F}_{\mathrm{rad}}$

Radiation force: $\mathbf{F}_{\mathrm{rad}} = \int \frac{\kappa_\nu}{c} \mathbf{F}_\nu \mathrm{d}\nu$

Self-gravitating hydrodynamics coupled to radiation transport and non-equilibrium chemistry. Relevant physics for galaxy formation: photoionization of atomic species, photodissociation of molecular species, heating of dust grains

Numerical challenges:
Use operator split to perform a radiation + chemistry step after the hydro and gravity step, the main time step being controlled by standard Courant conditions.
The radiation solver is used for radiation transport, but also for chemical evolution (HI, HII, H2 and metals) and gas cooling and heating: stiff source terms.

Dichotomy in the numerical methods: SPH versus mesh for hydro
Ray-tracing versus moment-based methods for radiation

- **(see Teyssier ANRAA review)**

Bibliography

- **Text books:**

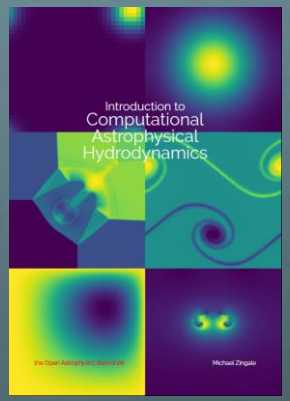

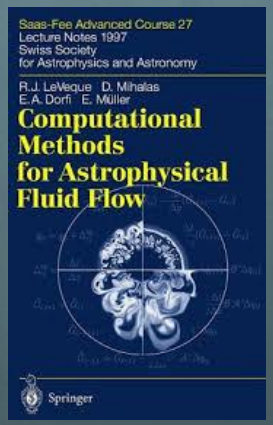

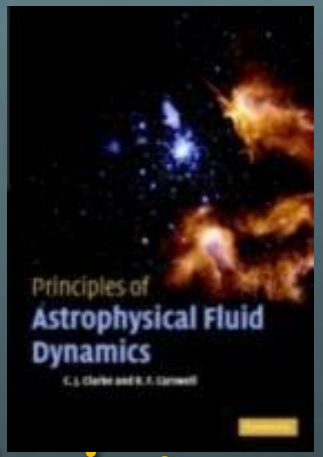

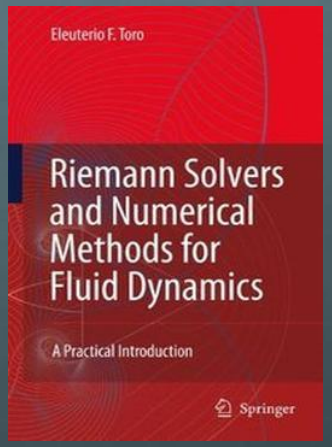

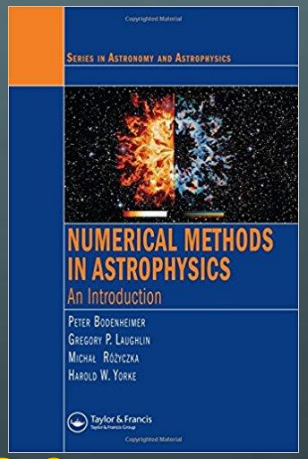

- https://archive.org/details/springer_10.1007-3-540-31632-9
- **A Primer on Eulerian Computational Fluid Dynamics for Astrophysics (arxiv/0210611)**
- Grid-Based Hydrodynamics in Astrophysical Fluid Flows (Teyssier, ANRAA, 53,325, 2015) (online in the Presentation's website)